Journal of Structural Geology 122 (2019) 116–132

Contents lists available at ScienceDirect

Journal of Structural Geology

journal homepage: www.elsevier.com/locate/jsg

# Style and timing of salt movement in the Persian Gulf basin, offshore Iran: Insights from halokinetic sequences adjacent to the Tonb-e-Bozorg salt diapir

Mohammad Ezati Asl[a], Ali Faghih[a,*], Soumyajit Mukherjee[b], Bahman Soleimany[c]

[a] Department of Earth Sciences, College of Sciences, Shiraz University, Shiraz, P.O. Box 71467-13565, Iran
[b] Department of Earth Sciences, Indian Institute of Technology Bombay, Powai, Mumbai 400 076, Maharashtra, India
[c] Research Institute of Petroleum Industry (RIPI), Tehran, Iran

ARTICLE INFO

*Keywords:*
Salt movement
Seismic interpretation
Growth strata
Halokinetic sequence
Persian Gulf
Iran

ABSTRACT

The variations in the rate of salt rise is reflected in the sedimentary sequences adjacent to salt diapirs and provides insights into the style of salt movement-sedimentation interaction and the timing of halokinetic phases. Episodic movement of salt diapir is defined by wedge- and tabular-shaped salt-related sedimentary strata (halokinetic sequences) adjacent to the diapir. Detailed mapping of depositional strata on 2D seismic sections adjacent to salt diapirs on the Tonb-e-Bozorg Island (Persian Gulf, SW Iran) reveals the presence of a series of sedimentary sequences related to the halokinetic activity of two salt source layers, the Hormuz and Fars salts, respectively. The Hormuz salt deposited in the uppermost Proterozoic, mobilized in the Lower Paleozoic and then continued to move periodically to present and to create the deep salt structures in the Tonb-e-Bozorg region. The Fars salt deposited in the Lower Miocene and then started rising, and created the central salt structure, the Tonb-e-Bozorg Island, and several peripheral ring-like salt structures around the island. Our results reveal that both the salt layers within the Tonb-e-Bozorg region grew by downbuilding and continued to move periodically by passive and active diapirism to the present. Salt movement-sedimentation interaction during salt diapirism influences petroleum play and therefore is of interest in petroleum geoscience.

## 1. Introduction

Creep/very slow flow of salts by differential loading is an important factor in the growth of salt structures. The movement of the salt body can create certain geometric features in their adjacent sequences. Accordingly, researchers have introduced several models and evolutionary stages for a salt structure (Trusheim, 1960; Vendeville and Jackson, 1992; Vendeville et al., 2002).

The sedimentary strata around a salt diapir detail the nature and the relative timing of diapirism (Giles and Rowan, 2012; Mohr et al., 2005; Giles and Rowan, 2012; Misra and Mukherjee, 2018; Wu et al., 2018a,b). The formation of a salt structure can play an important role in petroleum systems by controlling the style of sedimentation, the structural evolution of hydrocarbon traps, the thermal evolution of the sedimentary basin, and in shaping the migration pathways (Alsop et al., 2012; Hearon et al., 2014). Salt movements affect the surrounding sediments and create a halokinetic sequence (HS) *sensu* Giles and Lawton (2002).

The halokinetic sequence is characterized by relatively conformable sequences created from near-surface diapir or extrusive salt rise and bound by angular unconformity adjacent to the diapir, which becomes disconformable to conformable away from the salt body (Giles and Lawton, 2002). During slip-induced folding due to continued halokinesis, the degree of angular discordance increases at shallow depths (Rowan et al., 2003). The rate of salt rise versus the local sediment accumulation rate acts as a key factor in shaping the HS (Talbot, 1995; Giles and Lawton, 2002; Rowan et al., 2003; Giles and Rowan, 2012). Study of the relations between sediment accumulation rate and the rate of salt supply provides insight regarding the progressive evolution of the salt structures, the main time intervals of diapirism and the source layer depletion. The unconformity-bound halokinetic sequences are thinned, upturned and folded near passively growing diapirs (Giles and Rowan, 2012). Any locally unconformity-bound HS are thinned, upturned and drape folded near the passive diapirs. These interpretations come from outcrops, experimental modeling and seismic profile studies. The geometry of HS is controlled by the width of the strata. These

* Corresponding author.
*E-mail address:* afaghih@shirazu.ac.ir (A. Faghih).

https://doi.org/10.1016/j.jsg.2019.02.002
Received 11 August 2018; Received in revised form 6 February 2019; Accepted 7 February 2019
Available online 15 February 2019
0191-8141/ 

criteria provide two end-members of a spectrum of HS of two shapes: hook and wedge. Tabular and tapered composite halokinetic sequences (CHS) result from vertical stacking of hook and wedge-shaped HS. Tabular CHS results at a low ratio of rates of sediment-accumulation/diapir rise. Tapered CHS results under high ration of sediment-accumulation/diapir rise (Giles and Rowan, 2012).

Recent studies of HS emphasize their usefulness in distinguishing salt movement-sedimentation interaction and its influence on hydrocarbon-bearing traps (e.g. Poprawski et al., 2014, 2016). HS and angular unconformities reveal halokinetic movements and consequently episodes of salt diapirism. Seismic events such as truncations, onlaps, offlaps and pinch-outs around salt structures characterize the main episodes of salt movement (Giles and Lawton, 2002; Hudec and Jackson, 2007; Moraleda et al., 2015).

The evaporitic formations (e.g., Hormuz and Fars salt formations) at SE Zagros and Persian Gulf, have long been studied from academic and industrial angles (e.g. Harrison, 1930; Schroder, 1946; Kent, 1979; Gansser, 1960, 1992; Haffer et al., 1977; Letouzey et al., 2004; Sherkati et al., 2005, 2006; Sessegolo, 2006; Alsouki et al., 2008, 2011; Mukherjee et al., 2010; Mukherjee, 2011; Jahani et al., 2009, 2017; Callot et al., 2011; Motamedi et al., 2011; Soleimany et al., 2011; Trocmé et al., 2011; Perotti et al., 2016; Orang et al., 2018).

This study describes seismic, structural and stratigraphic attributes of strata deposited adjacent to the Tonb-e-Bozorg diapir in the eastern part of the Persian Gulf, southwest Iran (Fig. 1). To understand the relations between sedimentation and salt flow, HS geometries adjacent to the diapir are documented using two medium-resolution 2D seismic sections based on the geometric relationships between seismic reflectors and by characterizing the two types of HS: tubular and wedge types (Giles and Rowan, 2012). The main objective of this research is aimed at understanding:*(i)* geometric feature of stratigraphic sequences recording salt movement-sedimentation interaction during diapirism in the eastern parts of the Persian Gulf; and *(ii)* the timing of salt movement during the structural evolution of the Tonb-e-Bozorg salt diapir in particular.

## 2. Regional geology

The Persian Gulf is a foreland basin in front of the Zagros Fold-Thrust Belt along the northeastern margin of the African-Arabian Plate (Sharland et al., 2001; Alavi, 2004, Fig. 1). The Zagros Fold-Thrust Belt belongs to the Alpine-Himalayan orogenic system and resulted from the Cenozoic closure of the Neo-Tethys Paleo-Ocean (Alavi, 1994; Stampfli and Borel, 2002). The study area, the Tonb-e-Bozorg diapir, is located west of the Hormuz Strait (90 km away from the Hormuz Strait) in the eastern part of the Persian Gulf, SW Iran (Fig. 1).

Different tectonic events viz., rifting (Permian and Triassic), a passive continental margin setting in the Neo-Tethys paleo-ocean (Early Cretaceous- Jurassic), active continental margin setting and Late Cretaceous ophiolite emplacement and finally, approximately 200 km Neogene crustal shortening (Pirouz et al., 2017) and collision between the African-Arabian and the Central-Iranian plates produced the Zagros orogen (Berberian and King, 1981; Alavi, 1994). From bottom to top, the 8–12 km thick sedimentary succession includes:*(i)* the evaporites of the Hormuz salt as a main lower mobile group, *(ii)* the Cambrian Lalun sandstone to the Oligocene Asmari limestone as the competent group; *(iii)* the Lower Miocene evaporitic Gachsaran Formation including salt, anhydrite and marls as the main upper mobile group, and *(iv)* Plio-Pleistocene clastic deposits as the incompetent group. These tectonostratigraphic units produced several source-, reservoir- and cap rocks that constitute the richest petroleum province in the world (Konyuhov and Maleki, 2006). The extension resulted from the Late Proterozoic–Early Cambrian (570-530 Ma) Najd rifting produced N–S trending sub-basins, which controlled the distribution of the Hormuz salt in the northern part of the African-Arabian Plate (Sharland et al., 2001; Stampfli and Borel, 2004; Ghanadian et al., 2017a,b,c). The Hormuz Formation is the oldest known deposits in the Zagros and the Persian Gulf regions (Blanford, 1872; Pilgrim, 1908, 1924), which deposited on the basement (Ghazban, 2007). Several islands of the Persian Gulf, particularly in the west of Hormuz strait viz., the Abu Musa, Tonb-e-Bozorg, Larak and Hormuz owe their existence to the Hormuz salt. The Hormuz Formation deposited in the rift basins as syn-rift sediments (Kent, 1970), which were affected by the left-lateral strike-slip of the NW-SE trending Najd transform fault system (Loosveld et al., 1996; Al-Husseini, 2000). Its thickness decrease from the Zagros Mountain, which estimate 1.5–2.5 km, towards the Oman Mountains along N-S direction (Ghazban, 2007). Its thickness varies from 2 to 2.5 km in the study area and occurs at ~ 12 km depth (Kent, 1970; Al-Husseini, 2000; Ghazban, 2007).

The Hormuz Salt decoupled Zagros folding of the overlying sediments from its basement while also sourcing many salt domes (Kent, 1979; Talbot and Alavi, 1996; Edgell, 1992; Al-Husseini, 2000; Jahani et al., 2009; Soleimany et al., 2011; Motamedi et al., 2011; Buerberry et al., 2011). Late Permian-Early Triassic rifting changed the tectonic setting of the Persian Gulf, Zagros and Oman from an epicontinental to a passive continental margin of the Neo-Tethys Paleo-ocean (Stöcklin, 1968; Ricou, 1974; Stampfli and Borel, 2004). Gradual closing of the Neo-Tethys paleo-ocean and subduction started in the late Albian in Oman (Glennie, 2000; Sharland et al., 2001). This was followed by obduction of ophiolites over the continental lithosphere of the African-Arabian plate during the Late Cenomanian–Campanian (Béchennec et al., 1990; Searle et al., 2014). Regional uplift following this event developed a rapidly subsiding foreland basin in front of the uplifted Oman mountains (Glennie, 2000; Letouzey et al., 2004; Searle et al., 2014), which propagated towards the eastern part of the Persian Gulf (the study area) during Upper Cretaceous-Middle Miocene (Orang et al., 2018). A new foredeep basin in the centre of the eastern part of the Persian Gulf formed from Oligocene onward by a compressional orogeny in Oman (Boote et al., 1990; Searle et al., 2014). This allowed deposition of sediments equivalent to the Asmari Formation (Early Miocene) into two facies at sub-surface: *(i)* limestones of shallow-low energy marine environment to the west of the Hormuz strait and *(ii)* intercalations of Lower Miocene evaporitic claystones and anhydrites-the Fars Salt (Jahani et al., 2009) (Fig. 2).

## 3. Data and method

The data set used in this study has kindly been provided by the Iranian Offshore Oil Company (IOOC). The main block of data set consists of ~117 $km^2$ of 2D seismic data in a 2 × 2 $km^2$ regular grid together with well data, drill cuttings and logs obtained from exploration and development wells. The 2D seismic survey includes NE-SW lines of different lengths with a maximum ~200 km. The NW-SE lines are of different lengths with a maximum ~35 km. The seismic grid covers neither the Tonb-e-Bozorg Island nor the shallow waters around the island. This study uses Petrel software (2011.1 version) to characterize the local basinal salt structure.

Due to the absence of internal acoustic impedance contrasts in evaporites, seismic reflections are not expected from the salt. However, refraction and scattering of seismic ray paths travelling into and through the salt create noise that renders salt body boundary indeterminate (see Jackson and Hudec, 2017; Jones and Davison, 2014; Amin and Deriche, 2015 for seismic image-based diapir identification techniques). Considering these issues, the signal filtering attribute in the Petrel software was applied to enhance the resolution of the seismic images for better delineation of the salt body.

Detailed analyses of the three seismic transects, AA', BB' and CC' (Fig. 3a–d), along and across the study area, allowed the interpretation and correlation of key seismic reflections that derived the chronostratigraphy via exploration wells W2 and W3 (Fig. 3c). These wells are wildcats drilled in potential reservoir structures near the seismic section lines. The maximum depth of the wells drilled are into the Fahliyan

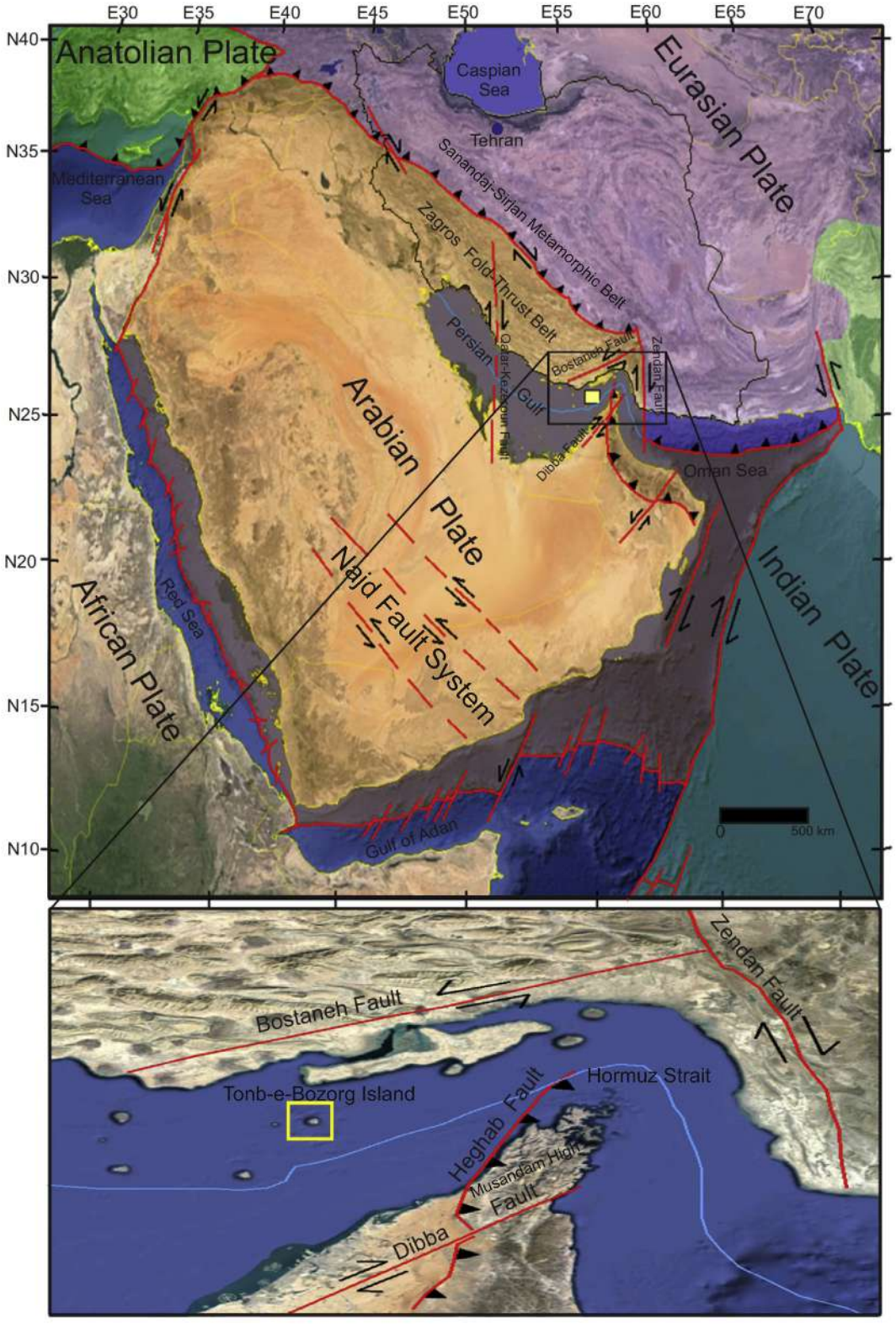


**Fig. 1.** Location and tectonic setting of the study area between the African-Arabian and Eurasian plates. The yellow rectangles outline the study area of the Tonb-e-Bozorg Diapir and Island in the eastern Persian Gulf. (For interpretation of the references to color in this figure legend, the reader is referred to the Web version of this article.)

Formation (Early Cretaceous). This led to recognizing different seismic facies and strata terminations, as well as major unconformities. The Two Way Time (TWT) structure maps show the present-day configuration of the interpreted seismic-stratigraphic horizons, some with known ages (Fig. 3d). Sixteen key horizons (including estimated top of the Hormuz Formation and the sea bed) from the Early Permian to present were picked up and tracked on the seismic sections (Figs. 4 and 5). Fig. 2 presents these horizons. The tops of the Devonian, Upper

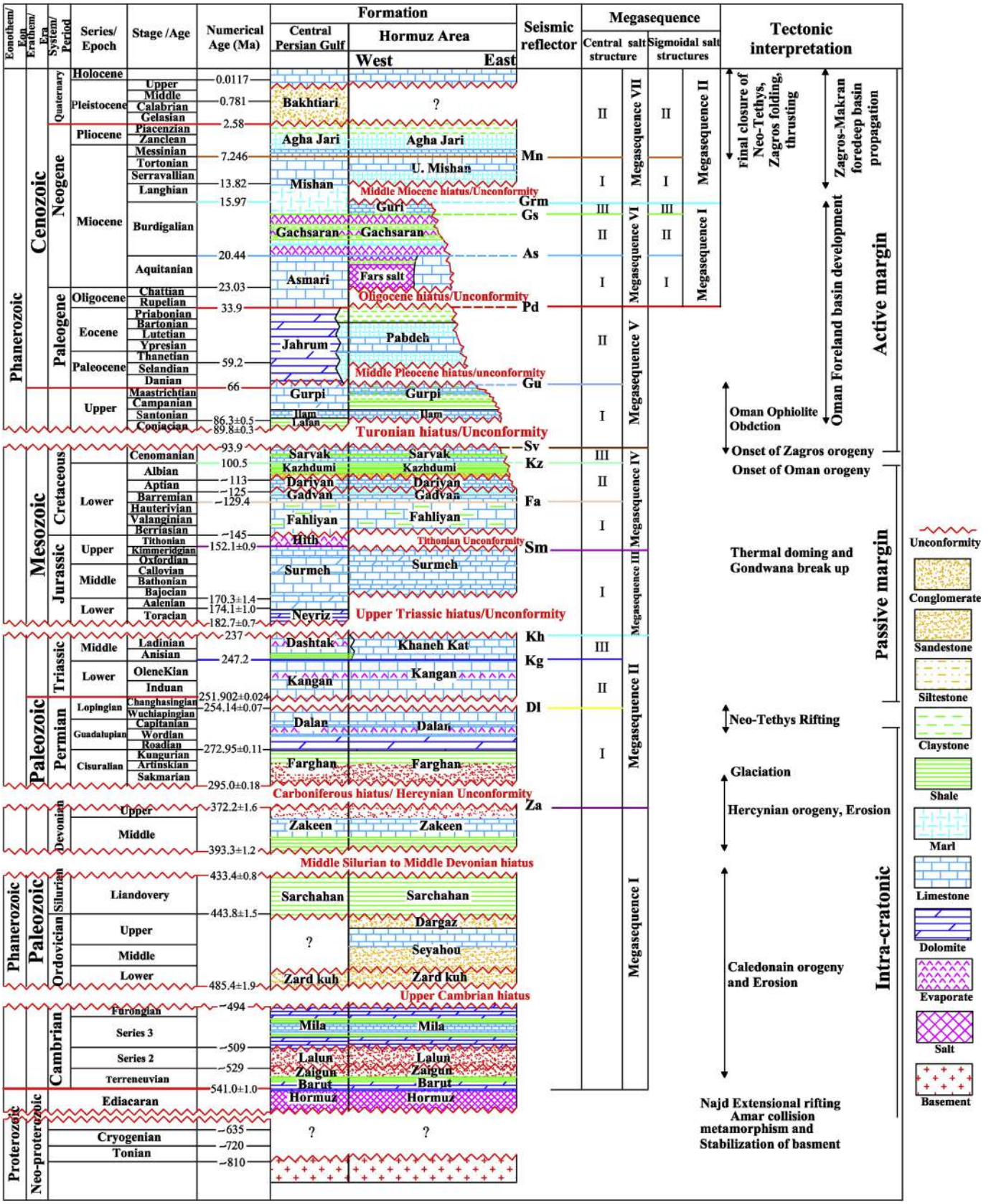


*(caption on next page)*

**Fig. 2.** Simplified lithostratigraphic column of the Hormuz strait in the eastern part of the Persian Gulf (modified after Gollesstaneh, 1965; Nayebi et al., 2000, 2001; Sharland et al. (2001); Ziegler, 2001; Ghavidel-Syooki, 2004; Alavi (2004);Ghazban (2007); Orang et al. (2018). The absolute age dates are based on the International Commission on Stratigraphy V 2017/02. The stratigraphic positions of interpreted seismic horizon reflectors and Megasequences defined in this study are shown. Abbreviations: (Mn) top Mishan (Middle-Late Miocene), (Grm) top Guri member (Early-Mid Miocene), (Mm) Middle Miocene unconformity Horizon, (Gs) top Gachsaran (Early Miocene), (As) top Asmari (Early Miocene), (Pd) top Pabdeh (late Paleocene-Eocene), (Ol) Oligocene unconformity Horizon, (Gu) top Gurpi (Maastrichtian-Early Paleocene), (Sv) top Sarvak (Cenomanian), (Tu) Turonian unconformity Horizon, (Kz), top Kazhdumi (Albian), (Fa) top Fahliyan (Early Cretaceous), (Sm) top Surmeh (Middle-Upper Jurassic), (Ti) Tithoniain unconformity Horizon, (Kh) top Khanehkat (Middle Triassic), (UT) Upper Triassic unconformity, (Kg) top Kangan (Early Triassic), (Dl) top Dalan (Late Permian), (He) Hercynian unconformity (Mid-Late Devonian).

Triassic, Tithonian, Turonian, Oligocene and Middle-Miocene sequences are all regional unconformities (e.g. Sharland et al., 2001; Ziegler, 2001; Ghavidel Syooki, 2004; Alavi, 2004; Letouzey et al., 2004; Orang et al., 2018) (Fig. 2). The lack of deeper wells, precludes study of formations below the Permian.

Decompaction and unfolding techniques were used to estimate the average sedimentation rate (Fig. 6) using the 2D Move software (version 2013, Midland Valley Ltd). The restoration has been applied by flattening of seismic reflectors on horizon following the geometric method presented by Gilardet et al. (2013) using the Petrel software. The decompaction procedure presumes that the initial porosity of the sediment at the time of sedimentation decreases progressively with burial (Schmoker and Halley, 1982). This procedure utilizes the exponential porosity/depth Athy'srelation $\emptyset_y = \emptyset_0 \exp^{-cy}$, (Athy, 1930). Here $\emptyset_y$: porosity at depth y, $\emptyset_0$: porosity of sediments at the surface, i.e., at y = 0; and c is an empirically derived lithology-dependent parameter. Note $c^{-1} = \lambda$ is called the "compaction constant". Standard values for $\emptyset_o$ and *c* have been used from the literature for rocks/sediments comprising the megasequences (Berra and Carminati, 2010, Table 1). Decompaction parameters for formations with multiple lithologies (Fig. 2) are calculated utilizing the porosity/depth coefficient (c) and the surface porosity ($\Phi_0$) values obtained from the ratio of lithologic percentages with their standard values (Table 2).

Decompaction was applied on the Permian (top of the Zakeen Formation) to Holocene succession. The underlying Paleozoic sequence was not unambiguously imaged by the seismic surveys and reach neither the crystalline basement nor the Hormuz Formation. Note that the pre-Permian sedimentary succession is essentially clastic and conglomeratic and probably is difficult to compact. The sequential 2D decompaction and unfolding techniques, start to remove loading of sea water or decompact and unfold the sea bed, i.e., the Holocene material. Then the next formation decompact and remove, and applying unfold

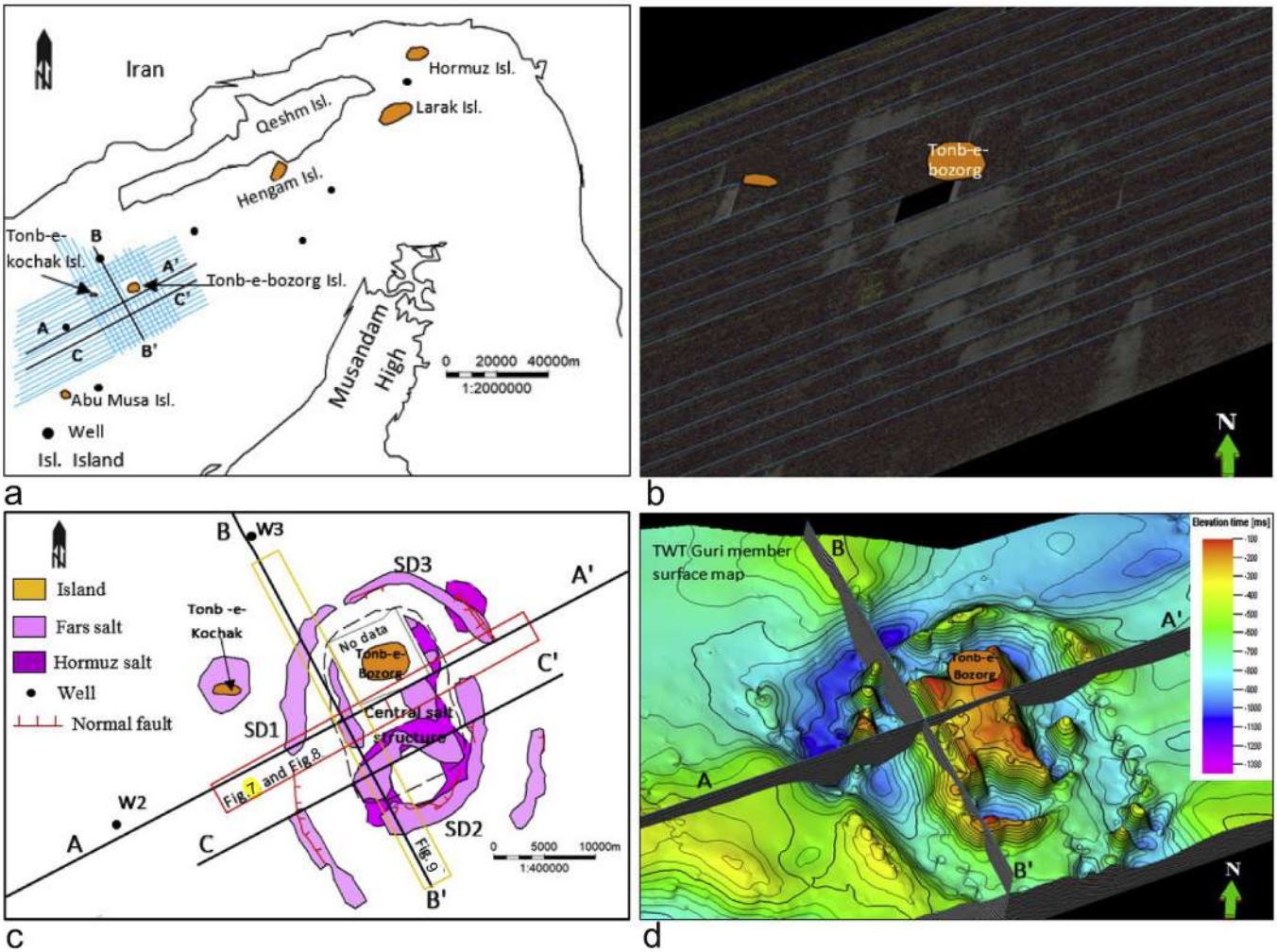


**Fig. 3.** a, b) Sketch map of the Tonb-e-Bozorg Island on the seismic sections. AA', BB' and CC' seismic sections trend NE-SW, NW-SE and NE-SW, respectively. c) Sketch map showing the location of Tonb-e-Bozorg Island and buried salt structures within the Tonb-e-Bozorg region, identified both as the Hormuz and the Fars salt bodies. Note locations of the exploration wells W2 and W3. d) TWT Guri member (Middle Miocene) surface map of the Tonb-e-Bozorg diapir.

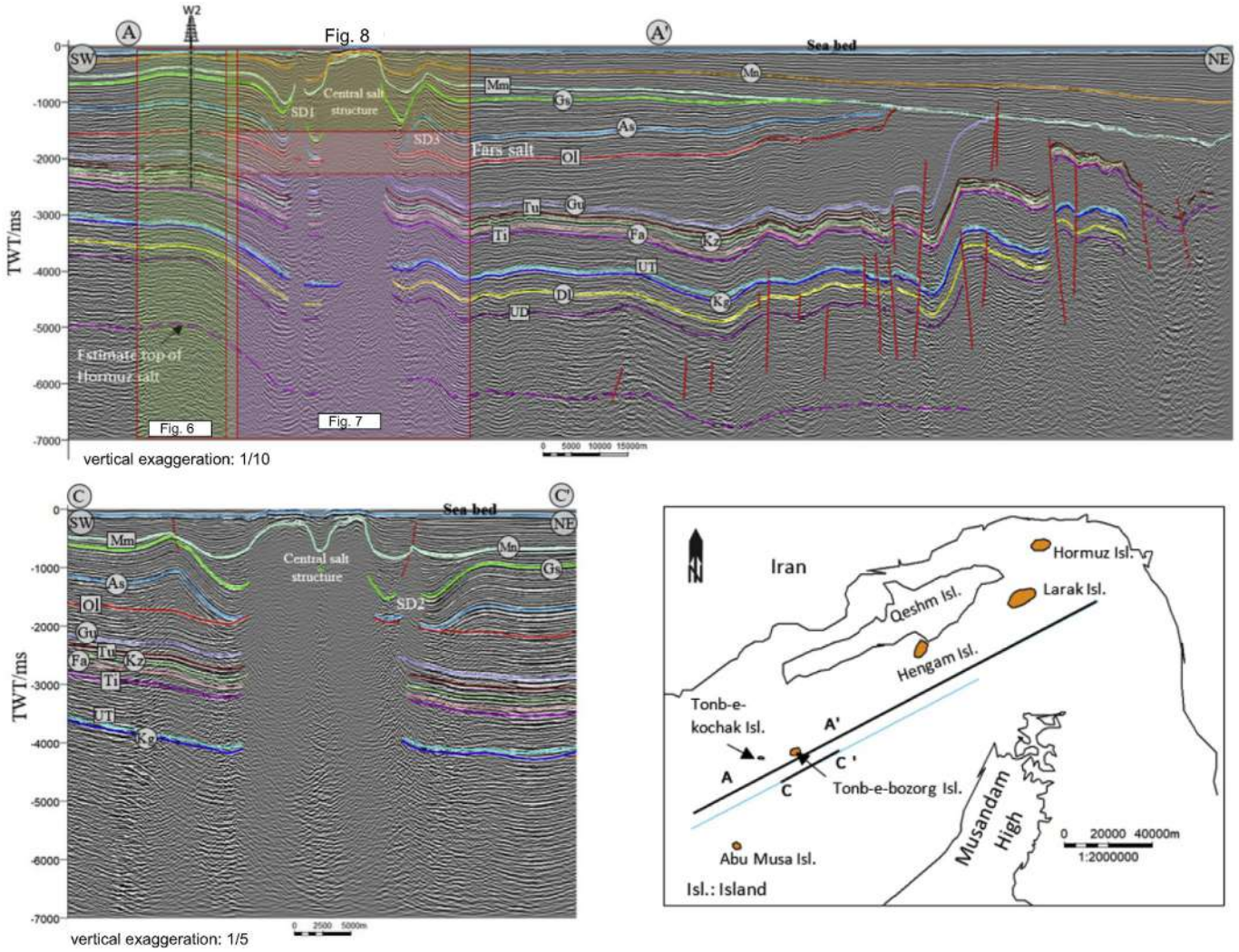


**Fig. 4.** Interpreted AA' and CC' seismic sections through the Tonb-e-Bozorg area. The interpreted SD1, SD3 and central salt structures and the location of seismic horizons (letters in circles) and major unconformities (letters in rectangles) are shown. Fig. 2 details abbreviations. Locations of Figs. 6–8 shown by colored columns. Vertical exaggeration: 1/10.

for next surface. This procedure has been repeated until the final units, the Dalan and the Faragun formations, are affected (Fig. 6).

Decompaction is a variable vertical enlargement that is a combination of heterogeneous vertical simple shear and positive dilatation (Rowan, 1993). We used homogeneous simple shear (e.g., Mukherjee, 2012) as the appropriate algorithm in unfolding in 2D Move software, (Midland Valley Ltd, 2013 version). The study area was depressed due to establishment of the Zagros foredeep basin during tectonic history. We choose the Airy Isostasy model (e.g., Mukherjee, 2017) in decompaction. However, the part of differential sedimentary loading across the region was balanced by changes in salt thickness of the Hormuz Formation. For each interval, calculated palaeowater depth in the Zagros basin and the present-day analogues were used (Table 2).

## 4. Results

### 4.1. Salt-related structures

Mapping results from interpretation of 2D seismic data display the present-day configuration of the salt structures within the Tonb-e-Bozorg region. Fig. 3c and d presents schematically the geometric configuration of salt structures (white areas on the seismic images). This distribution shows occurrence of a central salt structure including the Tonb-e-Bozorg island and several salt diapirs surrounded by ring-like diapiric ridge (e.g., SD1, SD2 and SD3, Figs. 4 and 5; see Amin and Deriche, 2015 for seismic image-based diapir identification techniques). The seismic features around the central structure reveals that it formed from two types of salt bodies:*(i)*the Hormuz salt that has created the deep salt structures; and *(ii)* shallow salt diapirs, which originated from the Fars source layer. Interpretation of seismic section show that the Hormuz salt body did not rise into the Pabdeh erosion level, but presence of igneous and metamorphic inclusions (Gansser, 1960) confirms that the Tonb-e-Bozorg salt diapir originate from the Hormuz salt. Presence of depression and circular rim syncline features, visible in the TWT surface map in the Guri member (Fig. 3d) around the central salt structure and weld points in the top of the Pabdeh horizon indicate that the Fars salt body inject into the central structure. Bending and depression of sedimentary sequences into the Fars deposits and presence of several weld points reveals that the ring-like salt structures originated from the Fars salt body. There is no evidence of salt movement below these rings and below the Late Paleocene- Oligocene strata of Pabdeh Formation.

### 4.2. Halokinetic sequences (HS)

Several HS were identified between the central and ring-like salt

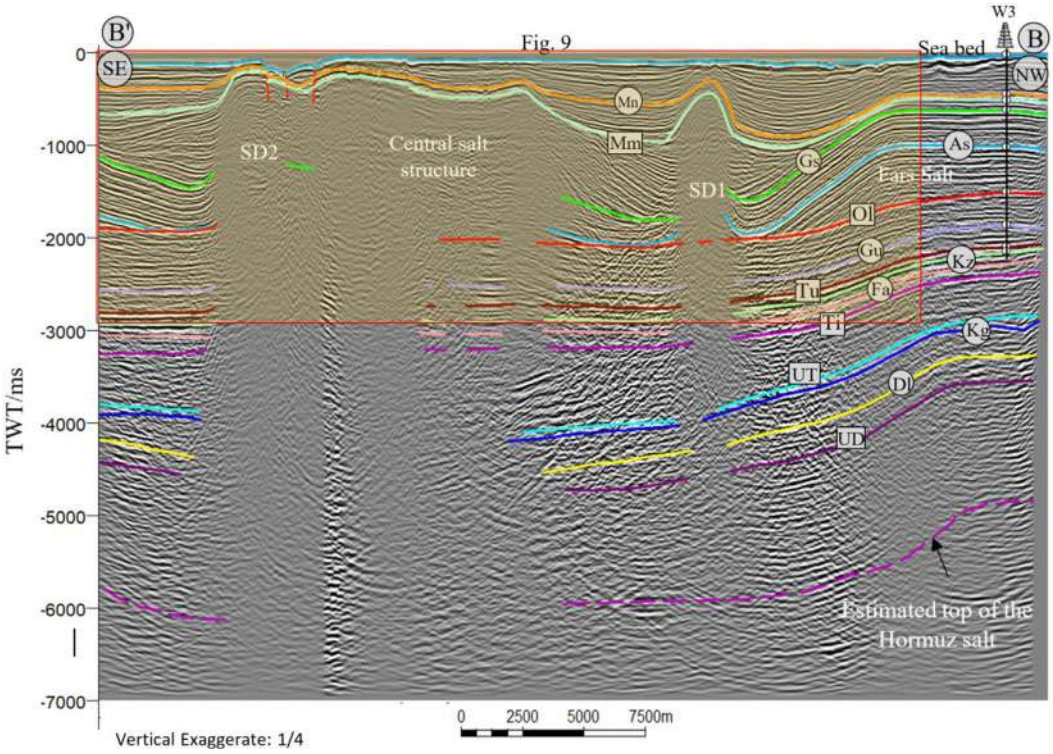


**Fig. 5.** Interpreted BB' seismic sections through the Tonb-e-Bozorg diapir. The interpreted SD1, SD2 and central salt structures and the location of seismic horizons (letters in circles) and major unconformities (letters in rectangles) are shown. Fig. 2 caption presents. Locations of Fig. 9 shown by colored columns. Vertical exaggeration: 1/4.

structures along the AA' and the BB' transects with ~4 km length along NE-SW and NW-SE directions, respectively. The boundaries of regional unconformities in the study area were the most important factors for defining the megasequences. These intervals (i.e. distance between two mutual unconformities) exhibit different sedimentation cycles and tectonic events affecting the evolving the salt structures. This approach has been adopted in other salt diapirs globally (e.g., Mohr et al., 2005, 2007; Giles and Rowan, 2012). Factors such as thickness variations and geometry distinguish several Megasequences adjacent to the central- and the ring-like diapirs.

*4.2.1. HS adjacent to the Tonb-e-Bozorg diapir along AA' section*

*4.2.1.1. Megasequence I.* This is the oldest Megasequence adjacent to the Tonb-e-Bozorg diapir (Figs. 2 and 7). Its top is a strong seismic event defined by the upper Devonian unconformity (top of Zakeen Formation) caused by the Hercynian event. Constrains in the resolution of our seismic data precluded recognition of its base. This Megasequence consists of the Cambrian to the base of the Permian sequences, which deposited on the Hormuz salt.

Most of the sequences are epi-continental silisiclastics deposited in the platform and continental margin environments in an intra-cratonic setting (Berberian and King, 1981). The sedimentation cycles were affected by the Caledonian and Hercynian events, which were followed by erosion and hiatus periods (Fig. 2). Low resolution seismic images preclude analyses of the halokinetic sequence in this interval (Fig. 7). Vague images of halokinetic sequence can be observed below the Upper Devonian unconformity, which indicate rising of the Hormuz salt body. Determination of timing and the factors affecting the flow of salt body are not possible (Discussions Section).

*4.2.1.2. Megasequence II.* This Megasequences is bounded by two strong seismic events: the Upper Devonian Unconformity at its base and the Upper Triassic Unconformity at its top (Figs. 2 and 7). It consists of the Permian to Middle Triassic deposits (Fig. 2) and is characterized by three seismic sequences.

S-directed subduction of the Paleo-Tethys began in the Late Carbonifer-Early Permian under the north margin of the Gondwanaland. This was followed by rifting of the Neo-Tethys Paleo-Ocean along the Main Zagros Fault and the Sanandaj-Sirjan metamorphic belt, SW Iran, in the Early and Middle Permian (Berberian and King, 1981; Sengör, 1990; Sharland et al., 2001, Stampfli and Borel, 2004). This tectonic system led to the Permo-Triassic opening of the Neo-Tethys Paleo-Ocean and associated regional extension and re-activated NW-SE trending planes into normal extensional and ~N-S/NNW-SSE trending wrench faulting.

The earliest extensive deposits following the Hercynian event were Lower Permian clastics, Faragun Formation, that were partly deposited coeval with rifting. The change of depositional environment caused by the tectonic activity into NW-SE extension, the Persian Gulf region come as rift basin by vertical movement whereby the greatest subsidence occurred at SE, i.e., the study area. This condition deposited carbonates in a ramp platform setting during transgressive and early highstand periods (e.g., the Khuff Formation in Oman and United Arab Emirates), and with intervening anhydrite beds during the late highstand periods, especially in the Late Permian, Dalan Formation (Iran). The Lower Triassic sequences consist of a succession of northeastward prograding interbedded evaporites and platform carbonates in shallow water environmental setting, the Kangan Formation. The Middle Triassic sequences are characterized by shallow-marine low-energy limestones toward the northeast, the Khaneh-Kat Formation. These sequences (i.e. Kangan and Khaneh-Kat formations) were deposited with a period of quiet sedimentation and minor tectonics.

The unconformity at the top of the Triassic carbonates probably resulted from warping up due to renewed rifting of the Neo-Tethys Paleo-Ocean or due to a eustatic sea level change (Murris, 1980). The dominance of regional extension phases has been accompanied by development of the sedimentary basin and sedimentation triggered the salt body. The presence and arrangement of probable halokinetic

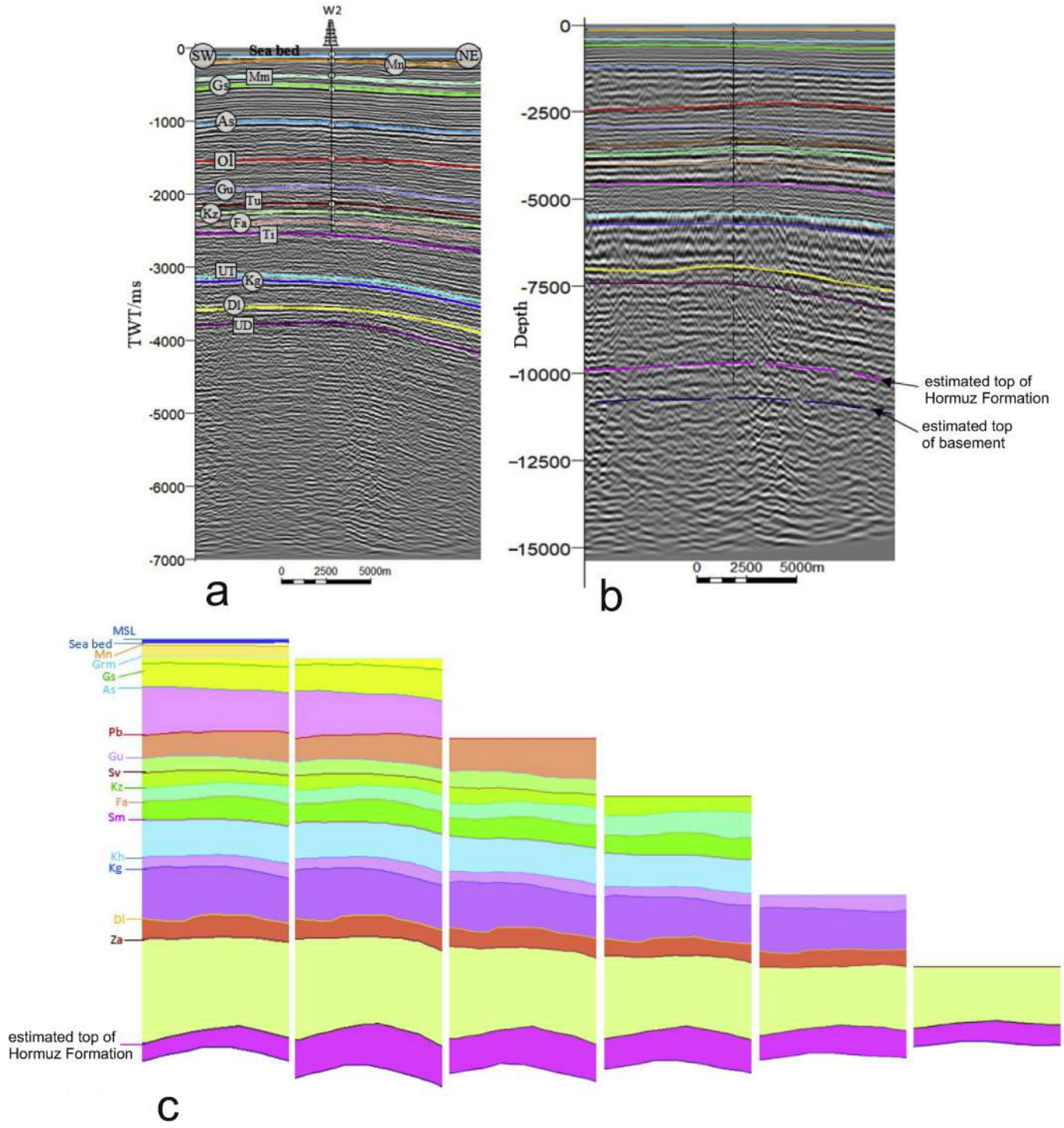


**Fig. 6.** Stages of decompaction and unfolding. a) TWT section, b) Depth section, c) sequential decompaction and unfolding.

sequences (Fig. 7) in this interval and absence of faults imply that the stimulation of the salt body depended on the sedimentation rate affected by regional tectonics. In extension intervals, the sedimentation rate was high and the wedge-shaped sequences formed. On the other hand, a slower sedimentation rate formed the tabular sequences.

*4.2.1.3. Megasequence III*. This Megasequence is bounded by two regional unconformities: an Upper Triassic unconformity at the base and a Tithonian unconformity at the top (Figs. 2 and 7). The Megasequence contains the Middle-Upper Jurassic Surmeh Formation, and is characterized by a single seismic sequence.

The onset of rifting of the India Paleo-Ocean from Africa-Arabian plate within the Gondwanaland in Early Jurassic (Rollinson et al., 2014) and spreading of the Neo-Tethys Palo-Ocean since Early Jurassic (Alavi, 2004) gradually attained the final stages. These resulted into subsidence and the creation of intra-shelf and inter-ramp basins along passive margin of the Neo-Tethys Palo-Ocean in the Jurassic. The Surmeh Formations (Middle-Upper Jurassic) is characterized by build-up of southwestward inter-ramp basin carbonates in a shallow-marine environment. The whole succession was capped by the deposition of the late highstand evaporite sequence, the Hith Formations (Tithonian). These evaporite deposits pinch out towards east and are not identified

**Table 1**
Original porosities and the decompaction coefficients of the single lithologies, from Berra and Carminati (2010).

| Lithology | Compaction Coefficient (c) | Porosity at the surface ($Ø_0$) | References |
|---|---|---|---|
| Conglomerates | 0 | 0.3 | Berra and Carminati (2010) |
| Sandstones | 0.2 | 0.49 | Sclater and Christie (1980) |
| Pelites (i.e. siltstones and shalestones) | 0.51 | 0.63 | Sclater and Christie (1980) |
| Micritic limestones (chalk) | 0.71 | 0.7 | Sclater and Christie (1980) |
| Limestones | 0.518 | 0.513 | Schmoker and Halley (1982) |
| Calcarenites (grainstones) | 0.25 | 0.445 | Goldhammer (1997) |
| Dolomites | 0.216 | 0.303 | Schmoker and Halley (1982) |
| Gypsum | 0.51 | 0.63 | Berra and Carminati (2010) |

**Table 2**
Decompaction parameters used in this study.

| Interval | Mean Thickness (m) and porosity recorded in wells | Lithology | Compaction Coefficient (c) | Surface Porosity ($Ø_o$) | Mean sedimentation (m)/ palaeowater | Mean rate of sedimentation (m/Ma) |
|---|---|---|---|---|---|---|
| Sea bed-top of Mishan (4.866 Ma) | 68 | 10% conglomerates<br>20% sand<br>50% Pelites<br>20% Limestone | 0.398 | 0.5456 | 72.83/(0) | ~14.96 |
| Top of Mishan-M.Miocene Un. (6.574 Ma) | 310 | 50% Pelites<br>50% Limestone | 0.514 | 0.5715 | 332.71/(10) | ~50.6 |
| M.Miocene Un.-top of Gachsaran (~1.2 Ma) | 142 | 10% Pelites<br>50% Limestone<br>40% Dolomite | 0.3964 | 0.4407 | 165.24/(15) | ~137.7 |
| top of Gachsaran- top of Asmari (~3.27 Ma) | 641 | 30% Pelites<br>10% Limestone<br>60% Gypsum | 0.5108 | 0.6183 | 796.79/(2) | ~243.67 |
| Top of Asmari-Oligocene Un. (~2.59 Ma) | 1041.5 | 5% Pelites<br>5% Gypsum<br>90% Salt | 0.00065 | 0.0001 | 1044.27/(5) | ~403.2 |
| Oligocene Un.- top of Gurpi (~25.3 Ma) | 615.5/32.5% | 80% Pelites<br>20% Limestone | 0.5116 | 0.6066 | 985.67/(30) | ~38.95 |
| Top of Gurpi-Turonian Un. (~20 Ma) | 356.5/25% | 40% Pelites<br>60% Limestone | 0.5148 | 0.5598 | 605.66/(200) | ~30.28 |
| Turonian Un.-top of Kazhdumi (~6.6 Ma) | 301.5/18% | 10% Pelites<br>90% Limestone | 0.5172 | 0.5247 | 508.71/(10) | ~77.07 |
| top of Kazhdumi-top of Fahliyan (~25 Ma) | 333/22.5% | 5% sand<br>35% Pelites<br>60% Limestone (ch) | 0.6145 | 0.8855 | 929.15/(30) | ~37.16 |
| Top of Fahliyan-Tithonian Un. (~15.6 Ma) | 589/20% | 90% Grainstone<br>10% Dolomite | 0.2466 | 0.4308 | 812.58/(10) | ~52.06 |
| Tithonian Un.-Upper Triassic Un. (~18.2 Ma) | 872 | 60% Limestone<br>40% Dolomite | 0.3972 | 0.429 | 1237.94/(150) | ~68 |
| Upper Triassic Un.-top of Kangan (~10.2 Ma) | 298 | 100% Limestone | 0.518 | 0.513 | 522.99/(15) | ~51.27 |
| top of Kangan-top of Dalan (~10.2 Ma) | 1197/15% | 45% Limestone<br>35% Dolomite<br>20% Gypsum | 0.4107 | 0.4629 | 1729.15/(15) | ~169.59 |
| top of Dalan-top of Zakeen (~40.6 Ma) | 536/15% | 20% sand<br>5% Pelites<br>10% Limestone<br>65% Dolomite<br>5% Gypsum | 0.2832 | 0.4092 | 799.84/(10) | ~19.7 |

in the north of the study area, (i.e. in the Qeshm Island, Jalali and Amiri, 1993) and top of the Surmeh Formation is characterized by the Tithonian Unconformity. This event resulted from subsiding of the northern margin of the Arabian plate towards the Neo-Tethys Paleo-Ocean.

The rise of salt at the beginning of this interval is characterized by sedimentary wedges truncated by seismic events close to the diapir. After that, the salt structure was buried during the accumulation of sediments, which further created wedge-shaped sequence indicating that the salt body rose near the time of the Upper Jurassic or Tithonian unconformity. These wedge-shaped sequences indicate rising salt body that folded the previous wedge and tabular sediments. The halokinetic sequences observed in the Megasequence III suggest that the salt moved in two episodes' coeval to sedimentation of the Surmeh Formation, first at the beginning and the at the end of the Jurassic (Figs. 2 and 7).

*4.2.1.4. Megasequence IV*. This Megasequence lies between the Tithonian and the Turonian unconformities at the bottom and top, respectively (Figs. 2 and 7). It consists of the Lower-Middle Cretaceous deposits: from the Fahliyan up to the Sarvak Formation (Fig. 2) and is characterized by three seismic sequences. The tabular sequences in this Megasequence indicate that the salt structure remained buried throughout sediment accumulation in this time interval. Thickness and low sedimentation rates accompanied by erosion periods and tectonic events had a less trigger affect on the salt rising rate.

During the Early Cretaceous, sedimentation begun with the deposition of shallow marine peloidal-oolitic limestone of the Fahliyan Formation of the Neocomian age (Nayebi et al., 2000, 2001) on open intra-shelf platform in the passive margin of the Neo-Tethys Paleo-Ocean (Sharland et al., 2001) associated with uplift. A general marine transgression allowed deposition of limestones and marls of the Gadvan

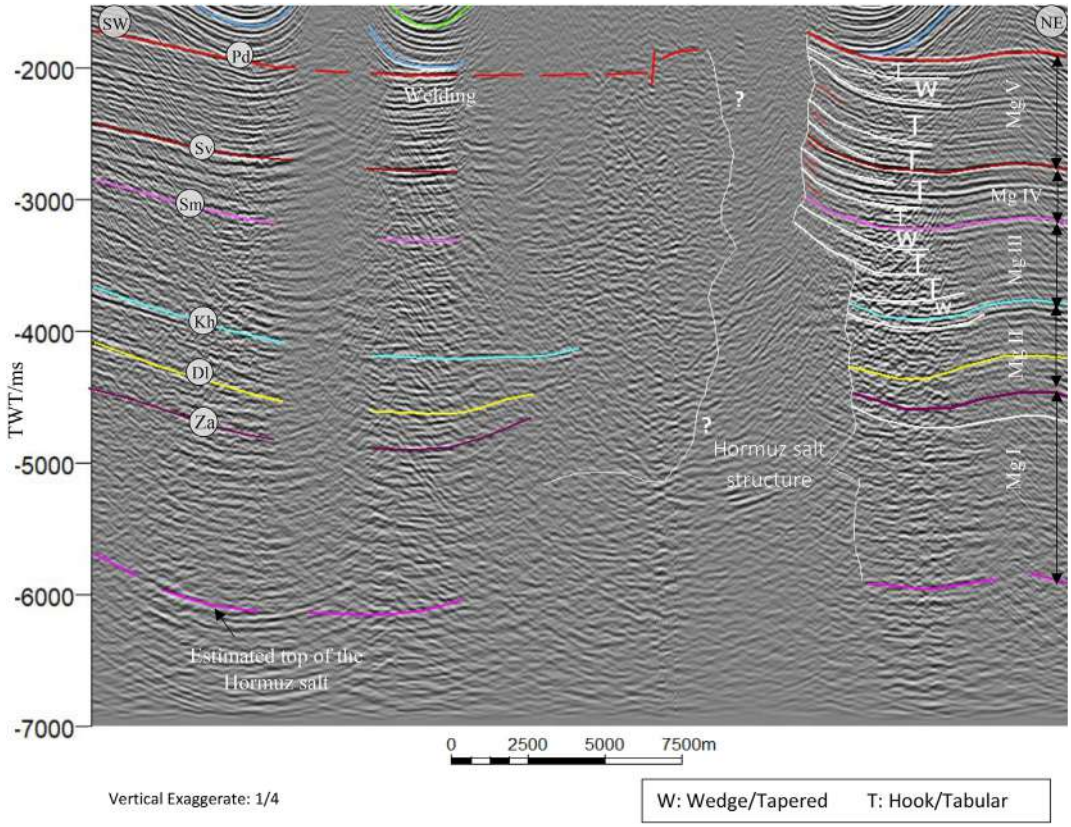


**Fig. 7.** Interpreted seismic sections showing development of HS on northeastern flank of the Central Salt Structure along the AA' seismic section (location is shown on Figs. 4 and 5). T, W letters: tabular and wedge-shaped HS, respectively. Fig. 2 caption presents abbreviations. Vertical exaggeration: 1/4.

Formation of Barremian to Aptian age (Nayebi et al., 2000, 2001). The shallowing of the sea during the Aptian deposited the Dariyan Formation with the Aptian age (Nayebi et al., 2000; 2001) with two facies: shallow-marine and deeper platform ramp.

Progressive uplift of the western Arabian plate, possibly *(i)* at the onset of spreading of the Atlantic Ocean floor in the Barremian times rotated the African-Arabian Plate anticlockwise, and *(ii)* onset of convergent to Eurasia in the Aptian–Albian (110–120 Ma) (Rollinson et al., 2014). These tectonic events changed the inherited northeastward tilting of the Arabian plate towards east and tilting into the Oman associated upwarping and creation of new sedimentary environments and migration of depocenters towards east (Loosveld et al., 1996; Al-Fares et al., 1998). These events in the study area developed an unconformity at the top of the Dariyan Formation (Aptian unconformity, Orang et al., 2018). The Albian sedimentation began with a major marine transgression, with widespread deposition of sandstone and deeper water shale of the Kazhdumi Formation of Albian-Cenomanian age (Nayebi et al., 2000, 2001). A general shallowing of the sea during the Late Albian and Cenomanian produced shallow marine carbonates, the Sarvak Formation, in the entire the area.

The African-Arabian and the Eurasia plates subducted the Neo-Tethys Paleo-Ocean under Eurasia, in Iran (Aptian-Coniacian, 115–85 Ma, Agard et al., 2011) and within Oman in the Early Cenomanian (Searle et al., 2014). Thus, the Oman area compressed and the southwestward obduction begun in the Early Cenomanian (Searle et al., 2014). The obduction of the Semail Ophiolites connotes a major period of structural inversion and uplift, downwarping, and tilting of the study area toward SE.

*4.2.1.5. Megasequence V.* The basal unconformity of Megasequence V is Turonian and the top unconformity is Oligocene (Figs. 2 and 7). This Megasequence contains Upper Cretaceous deposits, from the Ilam-up to the Pabdeh Formation (Fig. 2) and is characterized by two seismic sequences.

In the Late Cretaceous (Coniacian-Maastrichtian) further obduction of ophiolite resulted in the flexural loading and created a deep-water foreland basin in Oman (Suneinah foredeep basin: Boote et al., 1990; Aruma and Pabdeh foredeep basin in United Arab Emirate in north Oman: Ali et al., 2013). The propagation of tectonic movements towards Hormuz area established Gurpi and Pabdeh foredeep basins (Letouzey et al., 2004; Orang et al., 2018) and eastward tilting.

This transgression is represented by shale of the Laffan Formation (Coniacian) in the Persian Gulf and sedimentation continued with shallow marine carbonates of the Ilam Formation. A widespread marine transgression followed, which produced marls and shales of the Gurpi (Santonian-Early Paleocence, Nayebi et al., 2000, 2001) and Pabdeh Formation (Late Paleocence-Oligocene, Nayebi et al., 2000, 2001) in a for deep basin setting. The top of the Pabdeh Formation horizon indicates a truncated Oligocene unconformity in the study area (Letouzey et al., 2004; Orang et al., 2018) originated from collision of the Arabian Plate with the Iran-western Makran continental margin during the Late Oligocene–Early Miocene.

In the beginning of this period, the salt rise is indicated by tabular halokinetic sequences. The presence of sedimentary wedges in the upper parts of the Pabdeh Formation records a pulse of salt rise coeval to sedimentation. The effect of compressional phases in this interval is not well clear and presence of wedge-shaped sequences indicate change of rate of rising which can have originated from tectonic movements.

*4.2.2. HS adjacent to the shallow central salt structure along AA' section*

*4.2.2.1. Megasequence VI.* Megasequence VI is bounded by Oligocene and Middle Miocene unconformities in its base and top, respectively (Figs. 2 and 8). This Megasequence contains the Lower-Middle Miocene clastic deposits, the Fars salt to the Guri member and is characterized by

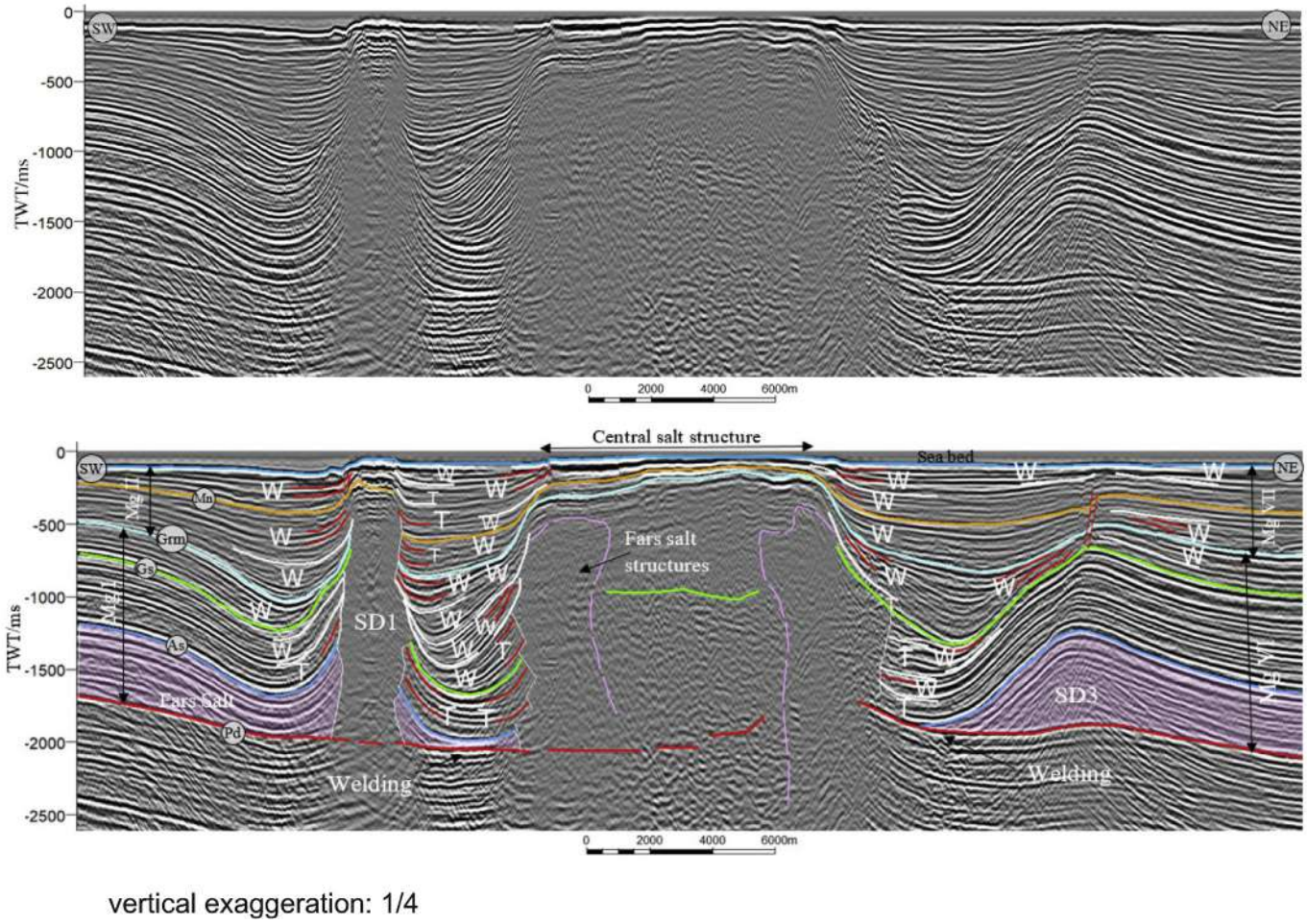


**Fig. 8.** Uninterpreted and interpreted seismic sections showing development of HS in the Central Salt Structures and ring-like salt structures, SD1and SD3, along the AA' seismic section (location in Fig. 4). T, W letters: tabular and wedge-shaped HS, respectively. Fig. 2 details abbreviations. Vertical exaggeration: 1/4.

three seismic sequences.

The new sediments, the Asmari Formation with Early Miocene age (Nayebi et al., 2000, 2001) deposited on the Oligocene unconformity surface with two different facies in a restricted basin related to the closure of the Hormuz Strait due to the Miocene uplift of the Oman Mountains (Jahani et al., 2009). Low-energy shallow marine limestones extend in the eastern part of the study area. Towards west within ~15 km, it laterally changes to an evaporite sequence, viz., the Fars salt (Kashfi, 1983) - a source for the Fars salt structures. Due to continuous NW compression in the north Oman, the lagoonal-evaporitic environments dominated and Early Miocene marl, limestone, shale, siltstone and gypsum of the Gachsaran Formation deposited (Nayebi et al., 2000). The Gachsaran deposits terminated with the marine transgression and deposition of the Early Miocene Guri member marls and reefal limestones (Nayebi et al., 2000) deposited at the base of the Mishan Formation. These sequences deposited in a concave basin and pinch out towards the uplifted eastern parts of the study area. The top of this sequence indicates a truncated Guri/intra-Mishan/Musandam unconformity (Letouzey et al., 2004; Orang et al., 2018).

The intervening tabular sequences have some internal thickness variations and are devoid of wedge-shaped strata. The presence of wedges in the lower parts of the Gachsaran Formation in the NE flank at the east salt structure (Fig. 8) indicates the onset of the Fars salt movement. The presence of wedge-shaped halokinetic sequences in the Guri member in the NE flank of the east salt structure indicates a pulse of rising salt body simultaneous with sedimentation with a rate lower than the sedimentation rate. The situation differs in the western flank of the salt structure. Wedge-shapes sequences are observed in the upper half of the Guri deposits. The other sequences, e.g., the lower half of the Guri member, are tabular.

*4.2.2.2. Megasequence VII.* The base of this Megasequence is at the Mid-Miocene unconformity and the top is the present sea floor of the Persian Gulf (Figs. 2 and 8). This Megasequence consists of Mid-Miocene to present-day deposits, from the Upper Mishan to the the Agha Jari Formation (Fig. 2) and is characterized by two seismic sequences.

Subsidence of the eastern parts of the study area as the Makran fold-thrust structures (Letouzey et al., 2004) propagated towards SW and deposited marl and limestone in the upper parts of the Early to Mid-Miocene Mishan Formation (Nayebi et al., 2000). These deposits gradually changed to the continental clastic Agha Jari Formation with age of the Late Miocene to Pliocene (Setudehnia, 1972). The Agha Jari Formation deposited in a marine environment in the lower parts and in a continental environment towards the top. This indicates a retrogression. These sequences thicken toward the eastern parts of the study area (Figs. 2 and 4). Sedimentary wedges truncated by seismic events close to salt structures characterize the entire thickness of this Megasequence. This indicates that the salt rose simultaneous to the sedimentation. The presence of wedge-shaped HS at the ends of this horizon indicates the present-day salt rise.

*4.2.3. HS adjacent to SD1 salt structure along AA' section*

*4.2.3.1. Megasequence I.* It lies between the two unconformities, Oligocene at the base and the Mid-Miocene at the top (Fig. 8). This

Megasequence contains the Lower to Mid-Miocene deposits, the Fars salt to the Guri member (Fig. 2), and is characterized by three seismic sequences. The distribution of wedge-shaped and tabular HS around the ring-like SD1 salt structure have different implications. The tabular sequence on the SW side of SD1 formed early in this interval and wedge-shaped sequences of growth strata date the end of this interval around the Mid-Miocene Unconformity marked by the sedimentation of the upper half of the Gachsaran Formation and all of the Guri member. By contrast, halokinetic sequences to the NE side of the SD1 salt structure include tabular sequences in the Gachsaran Formation and wedge-shaped halokinetic sequences in the Guri member. This stratal geometry indicates that the ratio of salt rise/sediment accumulation rates varied so that different sectors of the salt diapir grew at different rates.

*4.2.3.2. Megasequence II.* The Megasequence II lies between a basal Mid-Miocene unconformity and the present seafloor of the Persian Gulf (Fig. 8) and is characterized by two seismic sequences. The distributions of wedge-shaped and tabular HS around the ring-like SD1 salt structure also differ in this interval. To the SW flank of SD1, wedge-shaped HS occur at all of the interval while to the NE of SD1, it includes tabular and the wedge-shaped sequences occur only near the ends. Wedge-shaped HS in Megasequence II in the SW flank implies that the Fars Salt rose simultaneous during the interval of deposition. The salt body was buried during the interval at NE flank but rose again afterward. The presence of wedge-shaped HS at the ends of this interval indicate that the salt is still rising at present.

*4.2.4. HS adjacent to SD1 salt structure along BB' section*

*4.2.4.1. Megasequence I.* The Megasequence I lies between the Oligocene and the Mid-Miocene unconformities (Fig. 9). This Megasequence contains the Lower-Middle Miocene deposits, the Fars salt to the Guri member and is characterized by three seismic sequences. The time and pattern of salt movements in the SD1 salt structure differed in sections AA' and BB'. Halokinetic sequences in Megasequence I in the SD1 salt structure along the BB' section (Fig. 9) demonstrate that the initiation of salt movement differed on each flank and the rising of salt body was sooner in SE flank involving the Gachsaran Formation. Halokinetic sequences in the upper half of the Gachsaran Formation and lower parts of the Guri member indicate the salt mobilized during deposition of these sediments on the southeastern flank. By contrast, the salt body started rising on the NW flank during the ends of the Gachsaran Formation and the lower parts of sedimentation of the Guri member. In both the flanks, upward movement of salt body is characterized by tabular sequences.

*4.2.4.2. Megasequence II.* The basal Mid-Miocene unconformity and the present sea floor of the Persian Gulf are lower and upper boundaries of this megasequence, respectively. The upper parts of the Mishan to the sea bed sediments are characterized by two seismic sequences in the

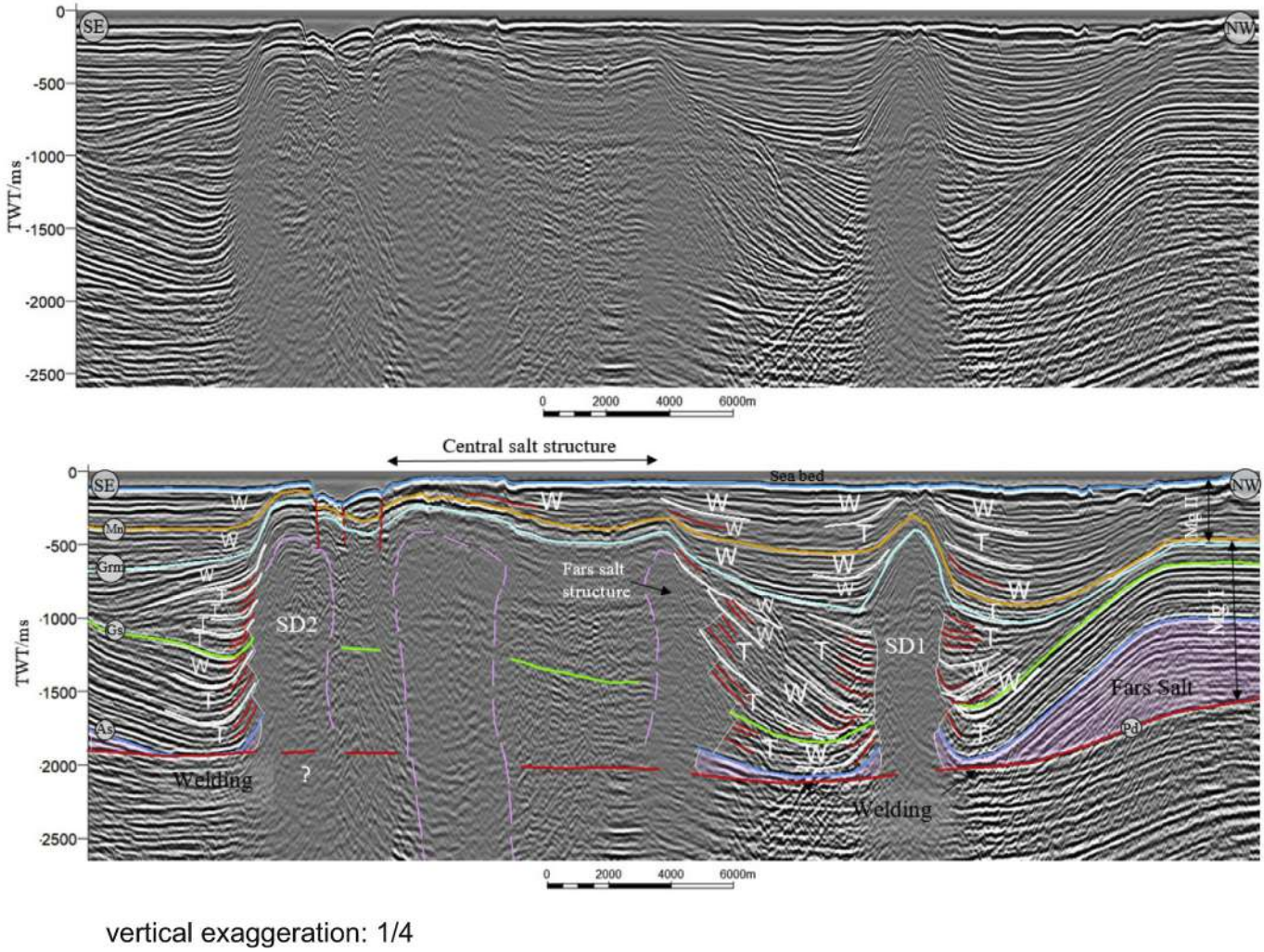


**Fig. 9.** Uninterpreted and interpreted seismic sections showing development of HS in the Central Salt Structure and ring-like salt structures, SD1and SD2, along the BB' seismic section (location shown in Fig. 5). T, W letters: tabular and wedge-shaped HS, respectively. Fig. 2 details abbreviations. Vertical exaggeration: 1/4.

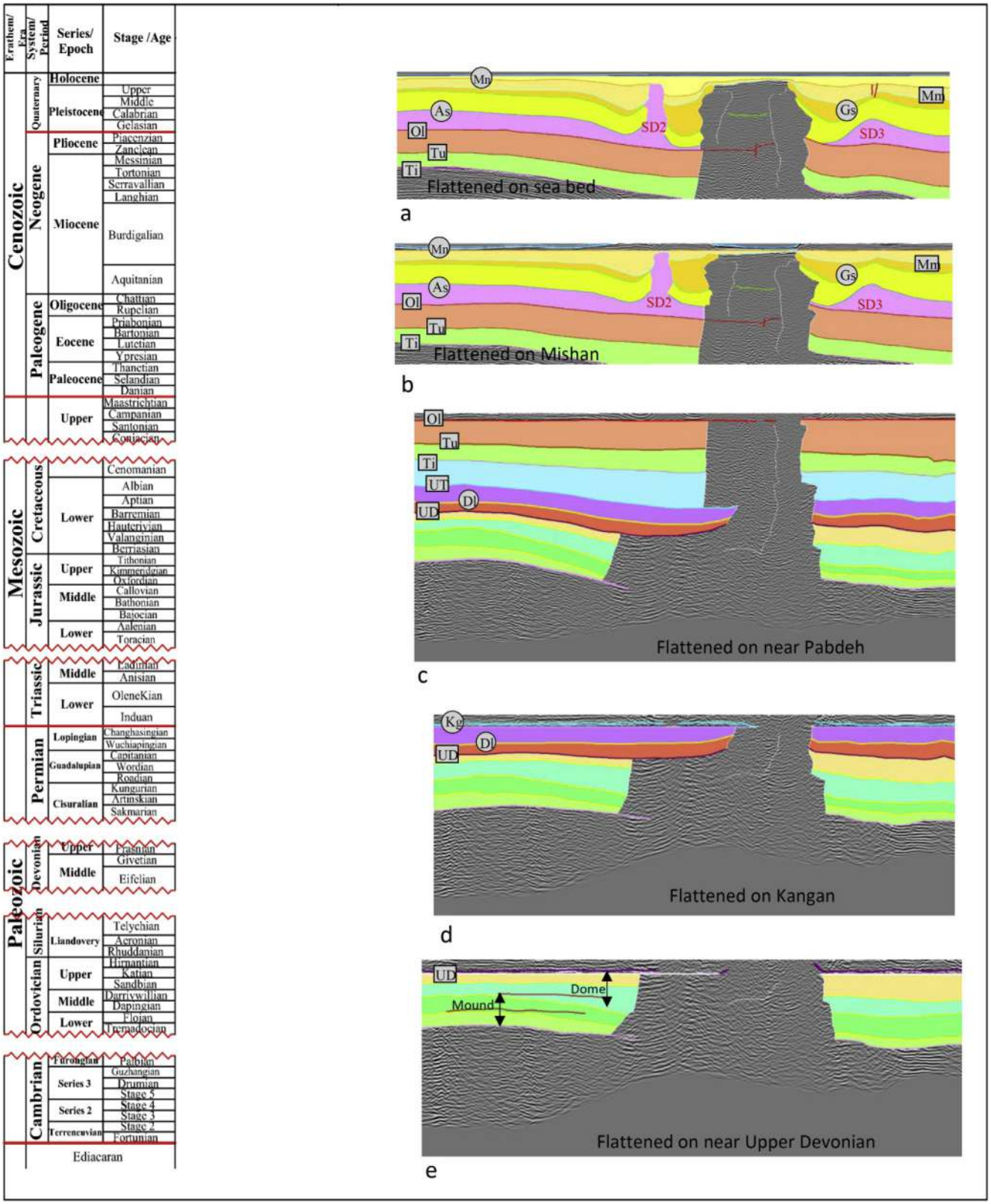


**Fig. 10.** Schematic presentation of the timing and evolution of Central and ring-like salt structures in the Tonb-e-Bozorg region. Uncertainties are due to low resolution of seismic data in this part of seismic section. Fig. 2 caption presents abbreviations. a) Welding in the Fars salt, start of post-dome stage in the Fars salt structures, continuation of the Fars salt rising until the Holocene, deposition of halokinetic wedge-shaped sequences, emergent of central salt structure and generation of Tonb-e-Bozorg Island. b) Deposition of Fars salt and its rise coeval to the Gachsaran and Guri sediments, development of rim syncline, injection of Fars salt into the Hormuz salt. c) Deposition until Oligocene unconformity, passive rise and withdrawal of the Hormuz salt as carbonates deposited up to the Turonian unconformity associated by hiatus, high rising rate in the Jurassic and diapir burial in the Cretaceous, high rising rate in the upper part of Pabdeh Formation, depression followed by withdrawal caused to increase the deposition and thickness of sediments in adjacent structure. d) Deposition up to the Upper Triassic unconformity associated with the rising salt, probably started to bury the diapir, welding and the post-dome stage. e) Deposition of Lower Paleozoic on the Hormuz salt, initiated rising of salt, the mound stage, the rim syncline, the dome stage, and deposition until the Upper Devonian unconformity.

Megasequence II. Wedge-shaped halokinetic sequences are more distributed on the SE flank of the SD1 salt structure than on its NW flank. Sedimentary wedges in this Megasequence reveal syn-diapiric deposition of the Mishan and the Agha Jari Formation on the SE flank. A single brief interval of interruption happened in the beginning of the Agha Jari Formation. On the NW flank of the structure, by contrast, salt started rising in the early and late stages of the sedimentation of the Agha Jari Formation. Sedimentation of the Mishan Formation buried the salt. Differing rates of sedimentary downbuilding around any diapir is likely to result in various geometries and tilts shown in vertical profiles.

#### 4.2.5. HS adjacent to SD2 salt structure along BB′ section

*4.2.5.1. Megasequence I.* This Megasequence contains the Lower to Mid-Miocene deposits (Fig. 9), the Fars salt to the Guri member and is characterized by three seismic sequences. HS in this Megasequence, mostly tabular, are only visible on the SE flank of SD2 salt structure. Wedge-shaped HS develop only in the last horizons and end of the Guri member. The initiation of salt movement coincided with sedimentation of the upper parts of the Gachsaran Formation.

*4.2.5.2. Megasequence II.* This Megasequence contains the Middle Miocene to present-day deposits (Fig. 9), the upper parts of the Mishan to the sea bed sediments and is characterized by two seismic sequences. Wedge-shaped sequences characterize the entire Megasequence II and are related to the SD2 salt structure devoid of tabular sequences. After a hiatus, the salt body resumed rising during sedimentation of upper parts of the Guri member and continued to rise during sedimentation of the upper parts of the Mishan to the Agha Jari Formation up to the present.

#### 4.2.6. HS adjacent to SD3 salt structure along AA′ section

*4.2.6.1. Megasequence I.* This Megasequence contains the Lower-Middle Miocene deposits (Fig. 8), the Fars salt to the Guri member, and three seismic sequences characterize it. The entire Gachsaran Formation is characterized by tabular HS; there is some evidence for wedge-shaped sequences at the last horizons in the SW flank. The wedge-shaped sequences can be observed in the both flanks of the salt structure in the Guri member, which indicates that the salt structure rose when the Guri member started depositing.

*4.2.6.2. Megasequence II.* This Megasequence contains the Middle Miocene to present-day deposits (Fig. 8), the upper parts of the Mishan to the sea sediments and is characterized by two seismic sequences. This Megasequence consists of wedge-shape HS related to the rise of the diapir in the lower and upper horizons of this interval. This distribution of HS indicates that the salt body was buried by the upper parts of the Mishan and lower parts of the Agha Jari Formation after a brief rise and again rose coeval to the sedimentation in the end of interval.

## 5. Discussions

### 5.1. Mechanisms of diapirism and timing of salt movement in the Tonb-e-Bozorg salt diapir

Due to low resolution of seismic images in depth and uncertain seismic stratigraphy below the upper Devonian horizon, there is no good evidence of the rising salt body, geometry of the basement, and sedimentation style adjacent to the root of deep the central salt structure. There is, however, some indirect evidence that partly reveals these issues. The salt-rock body is started deforming beyond a certain pressure threshold, usually between 50 and 150 bars, depending on its nature and composition (Cramz, 2006). The lower deformation threshold makes the salt rock plastic when stressed, even at(sub)surface conditions (Fossen, 2010) or behave like a viscous fluid in most geological conditions (Alsop et al., 2012) and even flow by a low stress cause by gravitational loading originate from weight of the adjacent rock pile (the Raleigh-Taylor instability). Theoretically, the salt rock body gradually can reach to the plastic threshold and undergo loading of weight exerted by 500 m of salt rock column at 300 m. Several seismic studies from the Atlantic margin in Brazil and Angola evidence for early salt flow/diapirism (Filbrandt et al., 2006; Quirk et al., 2012; Davison et al., 2012). The same is supported by the observations from ongoing salt flow in the Red Sea (Mitchell et al., 2010). Thus, a suitable 2–2.5 km thickness of the evaporative deposits of the Hormuz Formation allowed the salt body to reach the threshold of plastic deformation due to gravitational loading originated from salt body itself or lower thickness of the overburden. The evidence of sedimentation indicates continuously the Cambrian sedimentation on the Hormuz deposits, which can be another factor in stimulating salt flow.

Fig. 10 presents a model of the evolutionary stages of the central salt structure, where sections are obtained from flattening of seismic reflectors on the horizons. Comparison of cross-sections obtained from flattening near the upper Devonian horizon and the unflattened seismic image shows difference in the structural style and thickness in the flanks of the deep salt structure. This difference is more related to depress of the sequences in the western flank of structure, and also voluminous salt fed from this flank. These events could be evidence of the thickening of the Hormuz deposits in the western flank. Differential loading resulted from deposits on these evaporites explain the downbuilding process.

Anyway, when the salt flow started in this area was not well understood until drilling, but seismic data suggest that the diapirism of the Hormuz salt in the Zagros Mountains and in eastern part of the Persian Gulf began in the Early Paleozoic (e.g., Letouzey, et al., 2004; Jahani et al., 2009; Callot et al., 2011). Al-Barwani and McClay (2008) stated that the Ara Salt structures evolved through several deformation phases driven mainly by phases of sediment progradation from the W and NW. Differential loading is the most probable principal mechanism for initiating and driving halokinesis in the Hormuz Salt Basin in the Early Paleozoic. Motamedi et al. (2011) used seismic profiles, well data and field studies to find the timing of the first pulse of halokinetic movement of Hormuz salt to be pre-Silurian.

The increased thickness of the Hormuz deposits in the western flank can be due to the act of a (high-dip) normal fault below the central salt structure. This fault was active during the sedimentation of the Hormuz Formation. The difference in the thickness of sequences in the flanks of the deep central structure in the megasequence I, which is at a higher elevation in the western flank, can be due to the reactivation of this fault due to the Caledonian and Hercynian events. This caused withdrawal and rise of salt. However, interpretation of seismic sections shows that this fault slipped vertically. No faults were observed at the flanks that caused reactivation and growth of the salt structure. Also, in other megasequences, there is no evidence of faults causing lateral extension in the flanks of the deep salt structure, which causes salt extrusion. Hence, the salt body has grown more often by downbuilding processes that are activated and triggered by the tectonic regime. The difference in thickness of ~25 m along the line AA/, from 125 to 100 m, in the megasequence III shows an increase of withdrawal of the Hormuz salt from the western flank. In this period, extension phase dominated in study area and eventually the fault below the salt structure reacted possible as strike slip. Also, NW-SE sections show a thickening in this interval (Fig. 7). The thickness of the megasequences IV is low and has less inductive effect on the rising salt and has created a cap/roof. A similar condition also existed in the Megasequence V but due to sedimentation in a foredeep basin, the thickness of the deposits on the sides of the structure was not the same. In the semi-final sedimentation due to the domination of compression phase from the northern Oman with the orientation of the NW, the rising salt body folded the roof strata, connoting possibly an active diapiric stage. Folding resulted in an increase in the rate of rising salt body causes the

establishment of tubular and wedge-shaped halokinetic sequences in this megasequence.

The effect of tectonic loading on salt structures in the Zagros orogen has been discussed by many based on structural- and remote sensing studies. Some of them attribute the genesis and rise of diapirs to pull apart basins developing along the step-overs of N-S strike-slip fault zones. For example, Talbot and Alavi (1996) consider that diapirism along the Kazerun and Kar-e-Bas fault zones related to pull-apart basins formed at the step-overs along these two major strike-slip (transfer) faults within the Zagros. The rotation of basement blocks around vertical axes during strike-slip faulting can be one of the main reasons for salt rising into the diapirs (Hesami et al., 2001). Letouzey and Sherkati (2004), Callot et al. (2007) and Trocmé et al., (2011) mentioned evidence of salt movement prior to the main Zagros folding. The lateral pressure of the Neogene Zagros orogeny squeezed the salt to extrude and move downslope. The geometry of the HS adjacent to the studied salt structures shows that the salt body was moving long before the Zagros orogeny and downbuilding process can be one of the most important mechanisms for driving the diapirism. This mechanism is important within the evaporative basins of the world (Barton, 1933; Jenyon, 1986; Hudec and Jackson, 2007; Giles and Rowan, 2012). Protracted sedimentation can differentially load and downbuild a diapir (Barton, 1933), which depresses the surrounding sedimentary strata leaving the diapir crest close to the Earth surface (Rowan et al., 2003). The regional dip, progradation rate, sedimentation rate, primary salt thickness and overburden are important factors controlling salt movements (Jenyon, 1986). Instability could be due to inhomogeneity in the salt layer in its basement and/or in the overburden (Trusheim, 1960). Downbuild salt diapirs are signaled by halokinetic growth sequences in the adjacent source layer and changes in thickness that tilt nearby layers in the overburden. The absence of faults and nearby hook and wedge HS in and around the flanks of the salt structures in the Tonb-e-Bozorg region not only connote downbuilding but also confirms the criteria for recognizing passive diapirs detailed by Jackson et al. (1994), Rowan (1995) and Davison et al. (2000a, b).

Although many investigators have discussed the driving mechanisms of salt in the Zagros and Persian Gulf (e.g., Hesami et al., 2001; Letouzey and Sherkati, 2004; Callot et al., 2007; Koyi et al., 2008; Jahani et al., 2009), the timing of salt movement in these regions remains poorly understood. In most cases, the times of salt movement correlate with tectonics. The geometry of sedimentary strata adjacent to the any diapir dates the episodes of movement of its salt. The wedge-shaped and tabular HS adjacent to the salt structure date the intervals of its rise and burial.

Based on the changes in the thickness and geometric pattern of the strata adjacent to the central salt structure of Tonb-e-Bozorg region, the evolution of the structures can be divided into three stages (Fig. 10). Depression strata on the western flank of the salt structure in deep horizons within section which is flatten on upper Devonian indicates early withdrawal of the Hormuz source layer evaporitic bodies. This early motion was characterized by a gradual depression of the surrounding sediments in synforms, and accumulation of deposits in these basins associated with the first phase of the evolution of structure. The mound and dome stages are limited to the upper Devonian Unconformity and includes Precambrian and Lower-Middle Paleozoic deposits. Lack of deep exploration in the Persian Gulf basin means that we cannot date any of the pre-Permian sedimentary wedges. The deepest detected eventual wedge-shaped sequence, below the Upper Devonian horizon, recorded movement of salt. Most salt withdrawal occurred at the dome stage. Wedge-shaped sequences below the Hercynian Unconformity indicate the simultaneous mobility of the salt body with the sedimentation, which occurred repeatedly and could reflect the main tectonic phases in this region. The loading by later sedimentary cycles expelled the original salt body leading to nearby subsidence.

The “post-dome stage” began during Permian sedimentation and continued up to the present. Increased differential loading during sedimentation and tectonic caused upward movement of the salt body. The presence of wedge-shaped features in the Surmeh and Pabdeh Formation points out an increasing mobility of the salt body. The development of a foredeep basin due to the compression events of the Oman orogeny was the most important tectonic event after the Turonian. Sedimentation begun with the Fars salt and continued from the Neogene up to the present. Increased loading during sedimentation expelled the Fras salt further, which depressed the overburden and filled the ring-like basins around the Fars salt bodies. This situation continued until the Mid Miocene, Guri member. Expulsion of the Fars Salt lowered the depression and locally welded it to the base of the Fars source layer. This was prevented further expulsion of the Fars Salt bodies. Such subsidence created new spaces for Fars Salt accumulation as salt structures. Radial outward expulsion toward the Tonb-e-Bozorg central structures formed a surrounding ring-like salt structures. The age of further accumulation of Fars Salt in these new ring-like spaces, dates the salt movements. Until the Mid Miocene, some of these ring-like structures pierced the overburden and evolved into the dome stage. Compression due to Oman orogeny developed these salt structures, until the Mid-Miocene. The HS adjacent to the ring-like structures in the Fars Salt date when compression and differential load remobilized the salt. Some of the Fars Salt structures reaching the welding and dome stage got buried due to continuous sedimentation and passed post-dome stage. Buried salt domes indicate this. In most cases, the last HS adjacent to the salt structures are wedge-shaped. These reveal that recent movements of the salt body happened during the last phase of Zagros orogeny. The effects the propagation front of the Zagros folding is observed in the northern parts of the study area (Letouzey et al., 2004). The last compressive phase squeezed the major salt structure on the Tonb-e-Bozorg Island in the eastern part of the Persian Gulf.

## 6. Conclusions

The salt diapirs in the Tonb-e-Bozorg region were investigated to highlight a clear seismic image of the halokinetic sequences up to ~7 km depth into wedge-shaped and tabular in the salt withdrawal (or expulsion) basins, which were associated with passive and active stages of salt diapirism. The main mechanism for salt driving is differential loading induced by sediments downbuilding in local depo-centers. Interpretation of seismic sections and mapping of the geometry of HS revealed pulses of diapirism in the Tonb-e-Bozorg region. The Hormuz salt rose episodically in the Early Paleozoic before and during the Zagros orogeny. The other source layer, the Fars salt, rose creating the peripheral salt structures around the central Tonb-e- Bozorg salt diapir after Mid Miocene.

## Acknowledgments

We thank I. Alsop (Associated Editor, Journal of Structural Geology) for editorial handling. Constructive comments by P.A. Kukla and an anonymous reviewer improved the scientific content and presentation of the manuscript. Constructive comments by C.J. Talbot and J. Letouzey improved an earlier version of this manuscript. Support from the Shiraz University Research Council is acknowledged. SM was supported by CPDA grant of IIT Bombay. Special thanks to the Iranian Offshore Oil Company (IOOC) for providing the dataset, interpretation facilities and permission to publish the seismic data. Depth and thickness of horizons in the oilfield are the confidential data of the IOOC.

## References

Agard, P., Omrani, J., Jolivet, L., Whitechurch, H., Vrielynck, B., Spakman, W., Monie, P., Meyer, B., Wortel, R., 2011. Zagros orogeny: a subduction- dominated process. Geol. Mag. 148, 692–725.

Al-Barwani, B., McClay, K.R., 2008. Salt tectonics in the Thumrait area, in the southern part of the South Oman Basin: implications for mine-basin evolution. GeoArabia 13, 77–108.

Alavi, M., 2004. Regional stratigraphy of the Zagros fold-thrust belt of Iran and its proforeland evolution. Am. J. Sci. 304, 1–20.
Alavi, M., 1994. Tectonics of the Zagros orogenic belt of Iran: new data and interpretations. Tectonics 229, 211–238.
Al-Fares, A.A., Bouman, M., Jeans, P., 1998. A new look at the Middle to lower cretaceous stratigraphy, Offshore Kuwait. GeoArabia 3, 543–560.
Al-Husseini, M., 2000. Origin of the Arabian plate structures-amar collision and Najd rift. GeoArabia 5, 527–542.
Ali, M.Y., Watts, A.B., Searle, M.P., 2013. Seismic stratigraphy and subsidence history of the United Arab Emirates (UAE) rifted margin and overlying foreland basins. In: Chapter 13, Book Lithosphere Dynamics and Sedimentary Basins: the Arabian Plate and Analogues, pp. 127–143.
Alsop, G.I., Archer, S.G., Hartley, A.J., Grant, N.T., Hodgkinson, R., 2012. Salt tectonics, sediments and prospectivity: an introduction. In: In: Alsop, G.I., Archer, S.G., Hartley, A.J., Grant, N.T., Hodgkinson, R. (Eds.), 2012. Salt Tectonics, Sediments and Prospectivity, vol. 363. Geological Society of London, Special Publication, pp. 1–6.
Alsouki, M., Riahi, M.A., Abdollahie, F.M., 2008. Analysis of Moicene deposional systems in the Offshore area of Strait of Hormuz based on 3D seismic data. J. Appl. Sci. 8, 1812–1821.
Alsouki, M., Riahi, M.A., Yassaghi, A., 2011. Seismic imaging of sub-circular salt-related structures: evidence for passive diapirism in the Straits of Hormuz, Persian Gulf. Petrol. Geosci. 17, 101–107.
Athy, L.F., 1930. Density, porosity, and compaction of sedimentary rocks. AAPG Bull. 14, 1–22.
Amin, A., Deriche, M., 2015. A hybrid approach for salt dome detection in 2D and 3D seismic data. In: IEEE International Conference on Image Processing (ICIP), pp. 2537–2541.
Barton, D.C., 1933. Mechanics and formation of salt diapirs with special reference to Gulf coast diapirs of Texas and Louisiana. Bull. Am. Assoc. Pet. Geol. 17, 1025–1108.
Béchennec, F., LeMetour, J., Rabu, D., Bourdillon-de-Grissac, Ch, de Wever, P., Beurrier, M., Villey, M., 1990. The Hawasina nappes: stratigraphy, palaeogeography and structural evolution of a fragment of the south Tethyan passive continental margin. In: In: Robertson, A.F.H., Searle, M.P., Ries, A.C. (Eds.), The Geology and Tectonics of the Oman Region, vol. 49. Geological Society of London, Special Publication, pp. 213–223.
Berberian, M., King, G.C.P., 1981. Towards a paleogeography and tectonic evolution of Iran. Canada J. Earth Sci. 18, 210–265.
Berra, F., Carminati, E., 2010. Subsidence history from a backstripping analysis of the Permo- mesozoic succession of the central southern alps (northern Italy). Basin Res. 22, 952–975.
Blanford, W., 1872. Notes on the Geological Formations Seen along the Coast of Baluchistan and Persia from Karachi to the Head of the Persian Gulf and Some of the Gulf Islands. India: REC. Geological Survey of India.
Boote, D.R.D., Mou, D., Waite, R.I., 1990. Structural evolution of the Suneinah foreland, central Oman mountains. In: In: Robertson, A.H.F., Searle, M.P., Ries, A.C. (Eds.), The Geology and Tectonics of the Oman Region, vol. 49. Geological Society of London, Special Publication, pp. 397–418.
Buerberry, C.M., Jackson, C.A.L., Cosgrove, J.W., 2011. Late cretaceous to recent deformation related to inherited structures and subsequent compression within the Persian Gulf: a 2D seismic case study. J. Geol. Soc., Lond. 68, 485–498.
Callot, J., Jahani, S., Letouzey, J., 2007. The Role of Pre-existing Diapirs in Fold and Thrust Belt Development. Springer, pp. 309–325 (Chapter 16).
Callot, J.P., Trocme, V., Letouzey, J., Albouy, E., Jahani, S., Sherkati, S., 2011. Pre-existing salt structures and the folding of the Zagros mountains. Geol. Soc. Lond. Spec. Publ. 363, 545–561.
Cramz, C., 2006. Salt Tectonics Short Course. Universidade Fernando Pessoa.
Davison, I., Anderson, I., Nuttall, P., 2012. Salt deposition, loading and gravity drainage in the Campos and Santos salt basin. In: In: Alsop, G.I., Archer, S.G., Hartley, A.J., Grant, N.T., Hodgkinson, R. (Eds.), Salt Tectonic, Sediments and Prospectivity, vol. 363. Geological Society of London, Special Publication, pp. 159–174.
Davison, I., Alsop, G.I., Evans, N.G., Safaricz, M., 2000a. Overburden deformation patterns and mechanisms of salt diapir penetration in the Central Graben, North Sea. Mar. Petrol. Geol. 17, 601–618.
Davison, I., Alsop, G.I., Birch, P., Elders, C., Evans, N., Nicholson, H., Rorison, P., Wade, D., Woodward, J., Young, M., 2000b. Geometry and late-stage structural evolution of Central Graben salt diapirs, North Sea. Mar. Petrol. Geol. 499–522.
Edgell, H.S., 1992. Basement tectonics of Saudi Arabia as related to oil field structures. In: Rickard, M.H., others (Eds.), Basement Tectonics 9. Kluwer Academic Publishers, Dordrecht, The Netherlands, pp. 169–193.
Filbrandt, J.B., Al-Dhahab, S., Al-Habsy, A., Harris, K., Keating, J., Al-Mahruqi, S., Ismail Ozkaya, S., Richard, P.D., Robertson, T., 2006. Kinematic interpretation and structural evolution of North Oman, Block 6, since the Late Cretaceous and implications for timing of hydrocarbon migration into Cretaceous reservoirs. GeoArabia 11, 97–140.
Fossen, H., 2010. Structural Geology: Published in the United States of America. Cambridge University Press, New York.
Gansser, A., 1992. The enigma of the Persian salt dome inclusions. Eclogae Geol. Helv. 85, 825–846.
Gansser, A., 1960. ÜberSchlammvulkane und Salzdome, vol. 105. VirschrNaturforschGesel, Zurich, pp. 1–49.
Ghanadian, M., Faghih, A., Fard, I.A., Grasemann, B., Maleki, M., 2017a. Analogue modeling of the role of multi-level decollement layers on the geometry of orogenic wedge: an application to the Zagros Fold–Thrust Belt, SW Iran. Int. J. Earth Sci. 106 (8), 2837–2853.
Ghanadian, M., Faghih, A., Fard, I.A., Grasemann, B., Soleimany, B., Maleki, M., 2017b. Tectonic constraints for hydrocarbon targets in the Dezful Embayment, Zagros Fold and Thrust Belt, SW Iran. J. Petrol. Sci. Eng. 157, 1220–1228.
Ghanadian, M., Faghih, A., Fard, I.A., Kusky, T., Maleki, M., 2017c. On the role of incompetent strata in the structural evolution of the Zagros Fold-Thrust Belt, Dezful Embayment, Iran. Mar. Petrol. Geol. 81, 320–333.
Ghavidel-Syooki, M., 2004. Palynostratigraphy of Devonian sediments in the Zagros basin, southern Iran. Rev. Paleobot. Palynol. 127, 241–268.
Ghazban, F., 2007. Petroleum Geology of the Persian Gulf. Tehran University and National Iranian Oil Company.
Gilardet, M., Guillon, S., Jobard, B., Komatitsch, D., 2013. Seismic image restoration using nonlinear least squares shape optimization. In: International Conference on Computational Science, pp. 732–741.
Giles, K.A., Rowan, M.G., 2012. Concepts in halokinetic-sequence deformation and stratigraphy. In: In: Alsop, G.I., Archer, S.G., Hartley, A.J., Grant, N.T., Hodgkinson, R. (Eds.), Salt Tectonics, Sediments and Prospectivity, vol. 363. Geological Society of London, Special Publication, pp. 7–31.
Giles, K.A., Lawton, T.F., 2002. Halokinetic sequence stratigraphy adjacent to the El Papalotediapir, northeastern Mexico. AAPG Bull. 86, 823–840.
Glennie, K.W., 2000. Cretaceous tectonic evolution of Arabia's eastern plate margin: a tale of two oceans. In: In: Alsharan, A.S., Scott, R.W. (Eds.), Middle East Models of Jurassic/Cretaceous Carbonate Systems, vol. 69. Society of Economic Paleontologists and Mineralogists (SEPM), Spec. Publ, pp. 9–20.
Goldhammer, R.K., 1997. Compaction and decompaction algorithms for sedimentary carbonates. J. Sediment. Res. 67 (1), 26–35.
Gollesstaneh, A., 1965. A Micropaleontological Study of the Upper Jurassic and Lower Cretaceous of Southern Iran. Ph.D. thesis. Univ. London, London, pp. 629.
Haffer, J., Zardosht, H., Benyamin, N., 1977. The Regional Geology of the Strait of Hormuz, Southern Iran and Northern Oman. Hormuz Petroleum Company.
Harrison, J.V., 1930. The geology of some salt diapirs in Laristan. Quar. J. Geol. Soc. Lond. 86, 463–522.
Hearon, T.E., Rowan, M.G., Giles, K.A., Hart, W.H., 2014. Halokinetic deformation adjacent to the deep water Auger diapir, Garden Banks, 470, northern Gulf of Mexico: testing the applicability of an outcrop-based model using subsurface data. Interpretation 2, SM57–SM76.
Hesami, K., Koyi, H.A., Talbot, C.J., 2001. The significant of strike-slip faulting in the basement of Zagros fold and thrust belt. J. Petrol. Geol. 24, 5–28.
Hudec, M.R., Jackson, M.P.A., 2007. Terra Infirma, understanding salt tectonics. Earth Sci. Rev. 82, 1–28.
Jackson, M.P.A., Hudec, M.R., 2017. Salt Tectonic, Principles and practice Chapter 13 - Seismic Interpretation of Salt Structures. Cambridge University Press, pp. 364–398.
Jackson, M.P.A., Vendeville, B.C., Schultz-Ela, D.D., 1994. Structural dynamics of salt systems. Annu. Rev. Earth Planet Sci. 22, 93–117.
Jahani, S., Callot, J.P., letouzey, J., Frizon de Lamotte, D., 2009. The eastern termination of the Zagros fold and thrust belt (Iran): relationship between salt plugs, folding and faulting. Tectonics 28, TC6004.
Jahani, S., Hassanpour, J., Mohammadi-Firouz, S., Letouzey, J., Frizon de Lamotte, D., Alavi, S.A., Soleimany, B., 2017. Salt tectonics and tear faulting in the central part of the Zagros Fold-Thrust Belt, Zagros, Iran. Mar. Petrol. Geol. 86, 426–446.
Jalali, M.R., Amiri, F., 1993. Micropaleontology of Thin Section from Well Hulur#1 in Qeshm Island. National Iranian oil company report No, 1 (unpublished).
Jenyon, M.K., 1986. Salt Tectonics. Elsevier, Amsterdam 191pp.
Jones, I.F., Davison, I., 2014. Seismic imaging in and around salt bodies. SEG Interpret. 2 (4), SL1–SL20.
Kashfi, M.S., 1983. Variations in tectonics styles in the Zagros geo-syncline and their relation to the diapirism of salt in Southern Iran. J. Petrol. Geol. 6 (2), 195–206.
Kent, P.E., 1979. The emergent Hormuz salt plugs of southern Iran. J. Petrol. Geol. 2, 117–144.
Kent, P.E., 1970. The salt Plug of the Persian Gulf region. Leic. Lit. Philos. Soc. Trans. 64, 55–58.
Konyuhov, A.I., Maleki, B., 2006. The Persian Gulf Basin: geological history, sedimentary formations and petroleum potential. Lithol. Miner. Resour. 41, 344–361.
Koyi, H., Ghasemi, A., Hessami, K., Dietl, C., 2008. The mechanical relationship between strike-slip faults and salt diapirs in the Zagros fold- thrust belt. J. Geol. Soc. 165, 1031–1044.
Letouzey, j., Rocha, A., Furian, A., 2004. Major Tectonic Events and Structural Caractarisation of the Tusan Block. South Persian Gulf (report and presentations) (unpublished).
Letouzey, J., Sherkati, S., 2004. Salt movement, tectonic events, and structural style in the central Zagros fold and thrust belt (Iran). In: Salt Sediments Interactions and Hydrocarbon Prospectively, 24th Ann. GCSSEP Foundation, Bob F. Perkins research Conf.
Loosveld, R.J.H., Bell, A., Terken, J.J.M., 1996. The tectonic evolution of interior Oman. GeoArabia 1, 2851.
Mitchell, N.C., Ligi, M., Ferrante, V., Bonatti, E., Rutter, E., 2010. Submarine salt flows in the central Red Sea. Geol. Soc. Am. Bull. 122 (5–6), 701–713.
Misra, A.A., Mukherjee, S., 2018. Seismic structural analysis. In: Misra, A.A., Mukherjee, S. (Eds.), Atlas of Structural Geological Interpretation from Seismic Images. John Wiley & Sons Ltd, Hoboken, pp. 15–26 ISBN: 978-1-119-15832-5.
Mohr, M., Kukla, P.A., Urai, J.L., Bresser, G., 2005. Multiphase salt tectonic evolution in NW Germany: seismic interpretation and retro-deformation. Int. J. Earth Sci. 94, 917–940.
Mohr, M., Warren, J.K., Kukla, P.A., Urai, J.L., Irmen, A., 2007. Subsurface seismic record of salt glaciers in an extensional intracontinental setting (Late Triassic of NW Germany). Geology 35, 963–966.
Moraleda, L.A.R., Escalona, A., Schulte, L., Abdullah Sayghe, S., 2015. In: Interpretation, Modelling and Halokinetic Evolution of Salt Diapirs in the Nordkapp Basin 77th EAGE Conference and Exhibition.

Motamedi, H., Sepehr, M., Sherkati, S., Pourkermani, M., 2011. Multi-phase Hormuz salt diapirism in the southern Zagros, SW Iran. J. Petrol. Geol. 34, 29–44.
Mukherjee, S., 2011. Estimating the viscosity of rock bodies- a comparison between the Hormuz- and the Namakdan salt domes in the Persian Gulf, and the Tso Morari Gneiss dome in the Himalaya. J. Indian Geophys. Union 15, 161–170.
Mukherjee, S., 2012. Simple shear is not so simple! Kinematics and shear senses in Newtonian viscous simple shear zones. Geol. Mag. 149, 819–826.
Mukherjee, S., 2017. Airy's isostatic model: a proposal for a realistic case. Arab. J. Geosci. 10, 268. https://doi.org/10.1007/s12517-017-3050-9.
Mukherjee, S., Talbot, C.J., Koyi, H.A., 2010. Viscosity estimates of salt in the Hormuz and Namakdan salt diapirs, Persian Gulf. Geol. Mag. 147, 497–507.
Murris, R.J., 1980. Middle East: stratigraphic evolution and oil habitat. Am. Ass. Petrol. Geol. Bull. 64, 597–618.
Nayebi, Z., Bahrami, H., Ghavidel-syooki, M., 2001. Biostratigraphy and Micropalaeontology of the Cutting Samples from the Tusan Well-2. National Iranian oil Company, Exploration Directorate, Paleont NO-517 (unpublished).
Nayebi, Z., Bahrami, H., Ghavidel-syooki, M., 2000. Biostratigraphy and Micropalaeontology of the Cutting Samples from the Ashkan Well-1. National Iranian oil Company, Exploration Directorate, Paleont NO-508 (unpublished).
Orang, K., Motamedi, H., Azadikhah, A., Royatvand, M., 2018. Structural Framework and tectono-stratigraphic evolution of the eastern Persian Gulf, offshore Iran. Mar. Petrol. Geol. 91, 89–107.
Perotti, C., Chiariotti, L., Baresciani, I., Cattaneo, L., Toscani, G., 2016. Evolution and timing of salt diapirism in the Iranian sector of the Persian Gulf. Tectonophysics 679, 180–198.
Pilgrim, G.E., 1924. The geology of parts of the Persian provinces of Fars, Kerman and laristan. Memoir. Geol. Surv. India 48, 1–118.
Pilgrim, G.E., 1908. The geology of the Persian Gulf and the adjoining portions of Persia and Arabia. Memoir. Geol. Surv. India 34 (4), 1–177.
Pirouz, M., Avouac, J.-P., Gualandi, A., Hassanzadeh, J., Sternai, P., 2017. Flexural bending of the Zagros foreland basin. Geophys. J. Int. 210, 1659–1680.
Poprawski, Y., Basile, C., Agirrezabala, L., Jaillard, E., Gaudin, M., Jacquin, T., 2014. Sedimentary and structural record of the Albian growth of the Baikiodiapir (the Basque Country, northern Spain). Basin Res. 26, 746–766.
Poprawski, Y., Basile, C., Jaillard, E., Gaudin, M., Lopez, M., 2016. Halokinetic sequences in carbonate systems: An example from the Middle Albian Bakio Breccias Formation (Basque Country, Spain. Sediment. Geol. 334, 34–52.
Quirk, D.G., Schødt, N., Lassen, B., Ings, S.J., Hsu, D., Hirsch, K.K., Von Nicolai, C., 2012. Salt tectonics on passive margins: examples from Santos, Campos and Kwanza basins. Geol. Soc. Lond. Spec. Publ. 363 (1), 207–244.
Ricou, L.E., 1974. L'evolutiongeologique de la region de Neyriz (Zagross-Iranian etl'evolutionstructurale des Zagrides, vol. 1269 These univ.orsay. AD.
Rollinson, H.R., Searle, M.P., Abbasi, I.A., Al-Lazki, A., Al Kindi, M.H. (Eds.), 2014. Tectonic Evolution of the Oman Mountains. Geological Society, London, Special Publications 392p.368-369p.
Rowan, M.G., Lawton, T.F., Giles, K.A., Ratliff, R.A., 2003. Near-diapir deformation in La Popa basin, Mexico, and the northern Gulf of Mexico: a general model for passive diapirism. Am. Assoc. Petrol. Geol. Bull. 87, 733–756.
Rowan, M.G., 1995. Structural styles and evolution of allochthonous salt, Central Louisiana outer shelf and upper slope. In: In: Jackson, M.P.A., Roberts, D.G., Snelson, S. (Eds.), Salt Tectonics: a Global Perspective, vol. 65. AAPG Mem, pp. 199–228.
Rowan, M.G., 1993. A systematic technique for the sequential restoration of salt structures. Tectonophysics 228 (3–4), 331–348.
Schmoker, J.W., Halley, R.B., 1982. Carbonate porosity versus depth; a predictable relation for South Florida. AAPG Bull. 66 (12), 2561–2570.
Schroder, J., 1946. Géologie de l'ile de Larak. Contribution l'étude des dômes de sel du GolfePersique (Comparaison avec la Salt Range). Arch. Sci. Phys. Nat. 28, 5–18.
Sclater, J.G., Christie, P.A.F., 1980. Continental stretching: an explanation of the post-midcretaceous subsidence of the central north sea basin. J. Geophys. Res. 85 (B7), 3711–3739.
Searle, M.P., Cherry, G., Ali, M.A., Cooper, D.J.W., 2014. Tectonics of the Musandam Peninsula and northern Oman Mountains: from ophiolite obduction to continental collision. GeoArabia 19, 135–174.
Sengör, A.M.C., 1990. A new model for the late Paleozoic-Mesozoic tectonic evolution of Iran and implications for Oman. In: In: Robertson, A.H.F., Searle, M.P., Ries, A.C. (Eds.), The Geology and Tectonics of the Oman Region, vol. 29. Geological Society (London) Special Publication, pp. 797–831.
Sessegolo, L.A.-F., 2006. Regional Seismic Interpretation –Tusan Block, Persian Gulf, Iran. National Iranian oil company report, pp. 1–40 (unpublished).
Setudehnia, M., 1972. Iran du sud-ouest. In: LexiqueStratigraphique International HI, Fascicule 9b, Iran. Centre National de la Researche Scientifique, Pads, pp. 285–376.
Sharland, P.R., Archer, R., Casey, D.M., Davies, R.B., Hall, S.H., Heward, A.P., Horbury, A.D., Simmons, M.D., 2001. Gulf Petrolink. Arabian Plate Sequence Stratigraphy: Geo, vol. 2. Arabia Special Publication, Manama, Bahrain, pp. 371.
Sherkati, S., Molinaro, M., Frizon de Lamotte, D., Letouzey, J., 2005. Detachment folding in the Central and Eastern Zagros fold-belt (Iran): salt mobility, multiple detachments and late basement control. J. Struct. Geol. 27, 1680–1969.
Sherkati, S., Letouzey, J., Frizon de Lamotte, D., 2006. The Central Zagros fold-thrust belt (Iran): New insights from seismic data field observation and sandbox modelling. Tectonics 25. https://doi.org/10.1029/2004TC001766.
Soleimany, B., Poblet, J., Bulnes, M., Sàbat, F., 2011. Fold amplification history unrivalled from growth strata: the Dorood anticline, NW Persian Gulf. J. Geol. Soc., Lond. 168, 219–234.
Stampfli, G.M., Borel, G.D., 2004. The TransMed transects in space and time, constraints on the paleotectonic evolution of the Mediterranean domain. In: Cavazza, W., Roure, F., Spakman, W., Stampfli, G.M., Ziegler, P.A. (Eds.), TransMed Atlas. The Mediterranean Region from Crust to Mantle. Springer.
Stampfli, G., Borel, G.D., 2002. A plate tectonic model for the Paleozoic and Mesozoic constrained by dynamic plate boundaries and restored synthetic oceanic isochrons. Earth Planet. Sci. Lett. 196, 17–33.
Stöcklin, J., 1968. Structural history and tectonics of Iran: a review. AAPG Bull. 52, 1229–1258.
Talbot, C.J., 1995. Molding of salt diapirs by stiff overburdens in: salt Tectonics: a global perspective. In: In: Jackson, M.P.A. (Ed.), Amer. Assoc. Petrol. Geol. Memoir, vol. 65. pp. 61–67.
Talbot, C.J., Alavi, M., 1996. The past of a future syntaxis across the Zagros. In: In: Alsop, G.I., Blundell, D.J., Davison, I. (Eds.), Salt Tectonics, vol. 100. Spec. Publ., Geol. Soc., London, pp. 89–109.
Trocmé, V., Albouy, E., Callot, J.P., Letouzey, J., Rolland, N., Goodarzi, H., Jahani, S., 2011. 3D structural modelling of the southern Zagros fold-and-thrust belt diapiric province. Geol. Mag. 148, 879–900.
Trusheim, F., 1960. Mechanism of salt migration in northern Germany. AAPG Bull. 44, 1519–1540.
Vendeville, B.C., Jackson, M.P.A., 1992. The rise of diapirs during thin-skinned extension. Mar. Petrol. Geol. 9, 331–353.
Vendeville, B.C., John, A., Katherine, G., 2002. A new interpretation of Trusheim's classic model of salt-diapir growth. Gulf Coast. Assoc. Geol. Trans. 52, 943–952.
Wu, Z., Yin, H., Koyi, H.A., 2018a. Compressional salt-related structures in the western Quele area, Kuqa depression, Tarim basin, China. In: Misra, A.A., Mukherjee, S. (Eds.), Atlas of Structural Geological Interpretation from Seismic Images. John Wiley & Sons Ltd, Hoboken, pp. 163–166 ISBN: 978-1-119-15832-5.
Wu, Z., Yin, H., Koyi, H.A., 2018b. Reactive salt diapir, southern precaspian basin, middle Asia. In: Misra, A.A., Mukherjee, S. (Eds.), Atlas of Structural Geological Interpretation from Seismic Images. John Wiley & Sons Ltd, Hoboken, pp. 167–170 ISBN: 978-1-119-15832-5.
Ziegler, M.A., 2001. Late Permian to Holocene paleofacies evolution of the Arabian plate and its hydrocarbon occurrence. GeoArabia 6, 445–504.